

# **IMPROVEMENT IN PROCESS EFFICIENCY OF WAAM-TIG BY IN-SITU VOLTAGE–CURRENT– TEMPERATURE MONITORING AND FEEDBACK CONTROL SYSTEM**

**MS (Research) Thesis**

by

**ABNEESH KUMAR**

**(Roll No. 2304103002)**



**DISCIPLINE OF MECHANICAL ENGINEERING  
INDIAN INSTITUTE OF TECHNOLOGY INDORE  
APRIL 2025**



# **IMPROVEMENT IN PROCESS EFFICIENCY OF WAAM-TIG BY IN-SITU VOLTAGE–CURRENT– TEMPERATURE MONITORING AND FEEDBACK CONTROL SYSTEM**

**A THESIS**

*Submitted in fulfilment of the  
requirements for the award of the degree  
of*  
**Master of Science (Research)**

*by*

**ABNEESH KUMAR**

**(Roll No. 2304103002)**



**DISCIPLINE OF MECHANICAL ENGINEERING  
INDIAN INSTITUTE OF TECHNOLOGY INDORE**

**APRIL 2025**








# INDIAN INSTITUTE OF TECHNOLOGY INDORE

## CANDIDATE'S DECLARATION

I hereby certify that the work which is being presented in the thesis entitled **IMPROVEMENT IN PROCESS EFFICIENCY OF WAAM-TIG BY IN-SITU VOLTAGE CURRENT-TEMPERATURE MONITORING AND FEEDBACK CONTROL SYSTEM** in the fulfilment of the requirements for the award of the degree of **MASTER OF SCIENCE (RESEARCH)** and submitted in the **DISCIPLINE OF MECHANICAL ENGINEERING, Indian Institute of Technology Indore**, is an authentic record of my own work carried out during the time period from July 2023 to April 2025 under the supervision of **Dr. Yuvraj K Madhukar, Associate Professor, Indian Institute of Technology, Indore**.

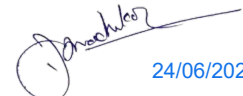
The matter presented in this thesis has not been submitted by me for the award of any other degree of this or any other institute.



24<sup>th</sup> June 2025

**Abneesh Kumar**

-----  
This is to certify that the above statement made by the candidate is correct to the best of my/our knowledge.



24/06/2025

Dr. Yuvraj Kumar Madhukar

**(Dr. Yuvraj K Madhukar)**


-----  
**Abneesh Kumar** has successfully given his/her MS (Research) Oral Examination held on 23<sup>rd</sup> June 2025



24/06/2025  
Dr. Santanu Manna  
Signature of Chairperson (OEB)



24-06-2025  
Signature of Convener, DPGC



Dr. Yuvraj Kumar Madhukar 24/06/2025  
Signature of Thesis Supervisor



Prof. Dhinakaran Shanmugam  
Signature of Head of Discipline  
June 24, 2025 HoD, MechE



## ACKNOWLEDGEMENTS

I sincerely express my heartfelt gratitude to my supervisor, **Dr. Yuvraj K. Madhukar**, for his invaluable guidance, continuous support, and inspiration throughout my research journey. I have been fortunate to have **Dr. Yuvraj K. Madhukar** as my supervisor. whose dedication to my work and prompt guidance have been invaluable. His hardworking and passionate approach to research, along with his commitment to achieving high-quality outcomes, has been a constant source of inspiration. Under his mentorship, I have been able to acquire, refine, and enhance my skills and scientific methodologies. His immense knowledge, guidance, observations, and comments helped me a lot to establish the overall direction of the research and to move forward with the investigation in depth. For all this, I will remain indebted and grateful to him for my entire life.

I am also grateful to the **Head of the Department, DPGC Convener**, faculty, and staff of the Department of Mechanical Engineering, IIT Indore, for providing a conducive research environment.

I would like to acknowledge **Prof. Suhas S. Joshi, Director, IIT Indore**, for providing a conducive environment for research and the opportunity to explore my research capabilities at IIT Indore. I am also thankful to **The Dean of Academic Affairs, The Dean of Research and Development, and The Dean of Student Affairs, IIT Indore**.

I sincerely thank the facility of Metallography and Tribology Lab, Computational Solid Mechanics Lab and Central Workshop, IIT Indore, for granting me access to various manufacturing and testing facilities.

I sincerely thank my seniors—Dr. Anas Ullah Khan, Mr. Shubham Sadhya, Mr. Arun Kumar Singh, and Mr. Mukulanand Jha—and my colleagues Mr. Vivek Ranjan Singh, Mr. Mohit Tiwari and Mr. Rushikesh Anil Mali for their constant support, collaboration, and the many memorable discussions we've shared. I am deeply grateful to my family for their unwavering support and blessings.

***-Abneesh Kumar***

Indian Institute of Technology Indore



**Dedicated To**

**My Beloved Family**

**Mother, father, and brothers for their unconditional love, blessings,  
and unwavering support.**



## ABSTRACT

This research work explores the development and implementation of a temperature-dependent feedback control system for Wire Arc Additive Manufacturing Utilising Tungsten Inert Gas (WAAM-TIG). The primary objectives were to enhance process efficiency, control bead geometry, and mitigate overheating, a common challenge in multilayer deposition. A Proportional–Integral–Derivative (PID) controller was employed to maintain the melt pool temperature at a desired setpoint behind the deposition point, thereby regulating bead geometry and improving the overall quality of fabricated parts.

The in-situ monitoring system ensured arc stability by adjusting input energy in real time, minimizing specific energy consumption and preventing overheating. This adaptive feedback control improved process efficiency by approximately 22%, enhancing WAAM-TIG deposition consistency.

Notable enhancements in bead geometry were achieved, with the bead height increasing by 27.1% and the bead width decreasing by 14.7%. This resulted in improved geometrical uniformity, a critical factor in ensuring the dimensional accuracy of additively manufactured components. Despite these improvements in process efficiency and geometry, the system exhibited a negligible impact on the mechanical properties of the deposited material, including tensile strength, hardness, and resultant microstructure.

The proposed control system enhances WAAM-TIG by ensuring real-time temperature regulation and arc stability, enabling reliable and efficient production. This advancement improves process control, promoting high-quality, energy-efficient, and precise metallic components for industrial applications.





## LIST OF PUBLICATIONS

### (A) Publications from MS (Research) thesis work

#### *In refereed journals*

1. **Abneesh Kumar**, S. Sadhya, A.U.Khan and Yuvraj K Madhukar, "Improvement in Process Efficiency of WAAM-TIG by In-Situ Voltage-Current-Temperature Monitoring and Feedback Control System", Int. J. Precis. Eng. Manuf. (2025). <https://doi.org/10.1007/s12541-024-01208-z>

### (B) Other publications during MS (Research)

#### *In refereed journals*

1. S. Sadhya, A. U. Khan, **Abneesh Kumar**, S. Chatterjee, and Y. K. Madhukar, "Development of concurrent multi wire feed mechanism for WAAM-TIG to enhance process efficiency," CIRP J Manuf Sci Technol, vol. 51, pp. 313–323, Jul. 2024, doi: 10.1016/j.cirpj.2024.04.010.

#### *In refereed conferences*

1. 13th International Conference on Precision, Meso, Micro and Nano Engineering: **Abneesh Kumar**, A K Singh, S. Sadhya, A. Kumrawat, M. Rama, Y. K Madhukar, "Methodologies to Fabricate strut structures using WAAM-MIG and associated mechanical responses," presented at the 13th Int. Conf. on Precision, Meso, Micro, and Nano Engineering (COPEN 13), Kozhikode, India, Dec. 13–15, 2024.
2. 13th International Conference on Precision, Meso, Micro and Nano Engineering: S. Sadhya, V. R. Singh, **Abneesh Kumar**, S. Chatterjee, and Y. K. Madhukar, "Dependency of Wire Feed Direction in TIG-Based Wire Arc Additive Manufacturing" presented at the 13th Int. Conf. on Precision, Meso, Micro, and Nano Engineering (COPEN 13), Kozhikode, India, Dec. 13–15, 2024.
3. 32nd DAE BRNS National Laser Symposium: V. R. Singh, **Abneesh Kumar**, N. Pandey, and I. A. Palani, "Investigating laser surface strategy to develop hydrophobic aluminium surface using microsecond pulsed Yb-doped fibre laser," in Proc. 32nd DAE BRNS Nat. Laser Symp. (NLS-32), Indore, India, 2024, pp. 548–551. Available: <https://www.ila.org.in/nls32>



# TABLE OF CONTENTS

<b>ABSTRACT</b>	<b>i</b>
<b>LIST OF PUBLICATIONS</b>	<b>iii</b>
<b>LIST OF FIGURES</b>	<b>ix-x</b>
<b>LIST OF TABLES</b>	<b>x</b>
<b>LIST OF ABBREVIATIONS AND SYMBOLS</b>	<b>xi</b>
<b>Chapter 1. Introduction</b>	<b>1</b>
1.1 Introduction to additive manufacturing (AM)	1-4
1.2 <b>Overview of key studies in WF-DED</b>	<b>4</b>
1.2.1 Wire-fed directed energy deposition (WF-DED) processes	4
1.2.2 Wire arc additive manufacturing (WAAM-TIG)	5
1.2.3 Wire arc additive manufacturing (WAAM-MIG)	5
1.2.4 Wire laser additive manufacturing (WLAM)	6
1.2.5 Other wire-based systems	6
1.3 Review of pertinent literature in in-situ monitoring and feedback control system	7-10
1.4 Objectives and scope of the thesis	10
1.5 Thesis Outline	11-12
<b>Chapter 2 Experimental setups and instrumentation</b>	<b>13</b>
2.1 Introduction	13
2.2 WAAM-TIG setup	14
2.2.1 Current measurement	14

2.2.2 Temperature measurement	15
2.2.3 Voltage measurement	16
2.3 Materials	16
2.4 Material characterisation	17
2.4.1 Sample preparation	17
2.4.2 Geometry analysis	17
2.4.2 Optical microscopy	18
2.4.3 Micro-indentation hardness	18
2.4.4 Strength analysis	19
<b>Chapter 3 In-situ voltage–current–temperature monitoring during WAAM-TIG</b>	<b>21</b>
3.1 Introduction	21
3.2 In-situ C-V-T monitoring during single-layer deposition	21
3.3 In-situ C-V-T monitoring during multi-layer wall deposition	22
3.3 Results and discussion	25
3.7 Summary	26
<b>Chapter 4 Implementation of temperature dependent feedback control system to improve the process efficiency of WAAM-TIG</b>	<b>27</b>
4.1 Introduction	27
4.2 Development and implementation of a PID-based feedback control system for WAAM-TIG	28-30

4.3 Results and discussion	31
4.4 Effect of feedback control system on process efficiency	31
4.5 Effect of feedback controller on various properties	32-38
4.6 Scalability analysis	38-39
4.7 Summary	40
 <b>Chapter 5 Conclusions</b>	 <b>41</b>
4.1 Major contributions	41
4.2 Future work	42
 <b>Reference</b>	 <b>43-45</b>



## LIST OF FIGURES

Figure No.	Caption	Page No.
1.1	Classification of additive manufacturing technologies (Hybrid Manufacturing Technologies, 2023)	2
1.2	Generic additive manufacturing process (Gibson et al., 2010).	4
1.3	Classification of directed energy deposition (DED) processes	5
1.4	(a) hall effect sensor (b) electronic circuit for voltage modification	8
1.5	Strategies for interlayer temperature measurement in thin wall WAAM: (a) Upper pyrometer strategy; and (b) sideward Pyrometer strategy	9
2.1	Schematic of WAAM-TIG system with installed different modules for in-situ monitoring of voltage, current and temperature.	14
2.2	Hall effect sensor-LA305-S	15
2.3	Pyrometer- IGAR-6	15
2.4	Schematic of sample locations for various analyses in a multilayer deposited wall	18
2.5	optical microscope	19
2.6	Vicker hardness tester	20
2.7	UTM setup for tensile	20
3.1	The recorded (a) voltage and current, and (b) temperature profile for single-layer bead deposition	22
3.2	The recorded (a) voltage and current, and (b) temperature profile for multilayer bead deposition	23
3.3	Schematic diagram of the heat dissipation modes, conduction ( $Q_{\text{cond}}$ ), convection ( $Q_{\text{conv}}$ ), radiation ( $Q_{\text{rad}}$ )	24
4.1	Logical flow chart of the closed-loop feedback control system.	29

4.2	The recorded (a) voltage and current, and (b) temperature profile for multilayer bead deposition with controller.	30
4.3	The obtained specific energy with the number of layers, with and without a controller	32
4.4	The obtained bead profile for multilayer wall and microscopic images across wall height for (a) with and (b) without controlled deposition	33
4.5	The obtained hardness behaviour with and without a controlled deposition	35
4.6	The (a) typical temperature profile and calculation for cooling rate, and (b) the obtained cooling rate with and without a controlled deposition.	36
4.7	The schematic and pictorial view of the test samples before and after the tensile test	37
4.8	The obtained stress-strain curve for multilayer deposited samples with and without a controller	38
4.9	Schematic diagram of geometry -1 and geometry-2	38

## LIST OF TABLES

<b>Table No.</b>	<b>Caption</b>	<b>Page No.</b>
2.1	Chemical composition of substrate plates and filler wire (ER70S-6)	16
4.1	Strength analysis test results	37
4.2	Scalability analysis of two different geometries	39



## LIST OF ABBREVIATIONS AND SYMBOLS

3D	Three Dimensional
AISI	American Iron and Steel Institute
AM	Additive Manufacturing
ASTM	American Society for Testing and Materials
BJ	Binder Jetting
CAD	Computer Aided Design
CAM	Computer Aided Manufacturing
CCD	Charged Coupled Device
CMT	Cold Metal Transfer
CWF	Cold Wire Feeder
DAQ	Data Acquisition
DED	Directed Energy Deposition
EBM	Electron Beam Melting
EDM	Electro Discharge Machining
GMAW	Gas Metal Arc Welding
GTAW	Gas Tungsten Arc Welding
ISO	International Organisation for Standardisation
WAAM	Wire Arc Additive Manufacturing
WAAM-MIG	Metal Inert Gas based Wire Arc Additive Manufacturing
WAAM-TIG	Tungsten Inert Gas based Wire Arc Additive Manufacturing
WAAM-PAW	Plasma Arc Welding based Wire Arc Additive Manufacturing
WF-DED	Wire fed Directed Energy Deposition
$wfs$	Wire Feed Speed
WLAM	Wire Laser Additive Manufacturing



# Chapter 1 Introduction

## 1.1 Introduction to additive manufacturing (AM)

Additive manufacturing is a layer-by-layer fabrication technology to produce three dimensional components. It has gained significant attention among designers, engineers, manufacturers, and researchers due to its innovative approach to fabricating three-dimensional components directly from CAD models. One of the key strengths of AM is its capability to produce complex geometries or highly intricate shapes that are difficult to fabricate using conventional manufacturing methods[1], [2] Additionally, this technology bridges the gap between digital design and physical realisation, enabling the production of customised and functional components directly from virtual models. The versatility and precision of additive manufacturing have made it an essential tool for fostering innovation and exploring creative solutions in engineering and design. This ability to directly translate virtual concepts into tangible products highlights the growing importance of additive manufacturing in modern industries [3].

Additive manufacturing (AM) processes, as classified under the ISO/ASTM 52900:2021 standard, which replaces ASTM F2792:2012, are categorised into seven types (Fig. 1.1): binder jetting, powder bed fusion, material extrusion, vat photopolymerization, directed energy deposition (DED), sheet lamination, and material jetting.

**Binder jetting (BJ)** involves using a liquid binding agent to bond layers of powdered material, forming the final object. This technique is compatible with materials such as metals, ceramics, and sand. Known for its efficiency and cost-effectiveness, binder jetting is particularly advantageous for producing large components at a high speed.

**Powder bed fusion (PBF)** technologies, including selective laser sintering (SLS), selective laser melting (SLM), and electron beam melting (EBM), use focused lasers or electron beams to selectively fuse powder particles in a bed. These processes support a wide variety of materials, including polymers, ceramics, and metals,

enabling the creation of complex parts with excellent mechanical properties and functional performance.

**Material extrusion**, represented by techniques like fused deposition modelling (FDM), involves the use of thermoplastic filaments. The filament is melted and deposited layer-by-layer through a heated nozzle to build the desired structure. Material extrusion processes are popular due to their affordability, versatility, and ease of use, making them accessible to a broad range of users.



Fig. 1.1: Classification of additive manufacturing technologies (Hybrid Manufacturing Technologies, 2023).

**Vat photopolymerization** encompasses methods such as stereolithography (SLA) and digital light processing (DLP), which cure liquid photopolymer resins layer-by-layer using lasers or projectors. These processes are renowned for their ability to deliver high-resolution components with smooth surface finishes, making them ideal for applications requiring precision.

**Directed energy deposition (DED)** employs focused energy sources, such as lasers, electron beams, or arcs, to melt and deposit material layer-by-layer. Both powder and wire can serve as feedstock for this process, which is commonly used in repair, surface cladding, and the production of large-scale components.

**Sheet lamination** involves bonding layers of adhesive-coated sheets, often made from materials like paper or metal, to construct the desired object. This category of additive manufacturing includes techniques such as laminated object manufacturing (LOM). Sheet lamination is known for its cost-effectiveness and the unique ability to combine different materials within a single build, making it suitable for diverse applications.

**Material jetting (MJ)** operates similarly to a traditional 2D inkjet printer but in a three-dimensional context. In this process, material is precisely deposited onto a build platform either continuously or using a drop-on-demand (DOD) method. Each layer is solidified using ultraviolet (UV) light to form the final structure. The materials compatible with this technique are limited, as they must have a viscosity that allows for droplet formation. Polymers and waxes are the most used materials due to their suitability for the process.

This classification highlights the diversity of additive manufacturing technologies, each suited to specific applications and material requirements.

In recent years, numerous additive manufacturing (AM) processes have been developed, yet they all follow a similar fundamental workflow (Fig. 1.2). The process starts with creating a computer-aided design (CAD) model, which acts as the digital blueprint of the object to be manufactured. Once the CAD model is complete, it is converted into an STL (Standard Tessellation Language) file. This file format represents the geometry of the object by breaking it down into a series of interconnected triangles.

Specific parameters, such as layer thickness and infill density, are assigned to each layer during the preparation stage. This step generates the necessary instructions for the additive manufacturing (AM) system, enabling it to construct the object layer by layer.

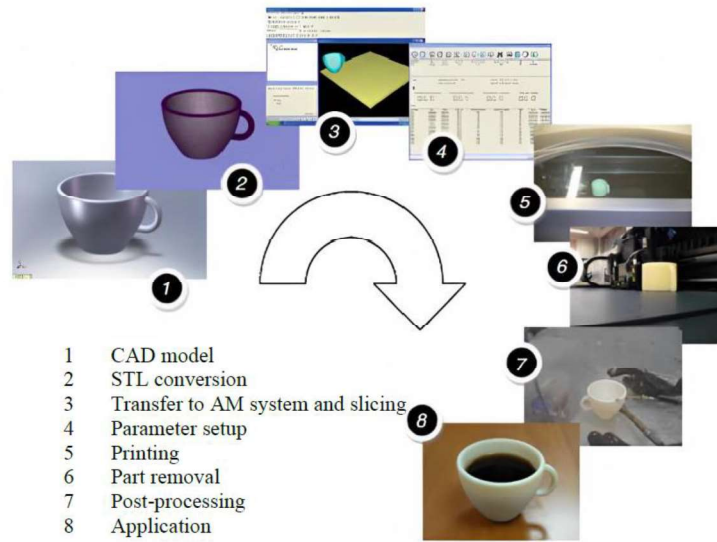


Fig. 1.2: Generic additive manufacturing process (Gibson et al., 2010).[4]

## 1.2 Overview of key studies in WF-DED

### 1.2.1 Wire-fed directed energy deposition (WF-DED) processes

Wire-fed directed energy deposition (WF-DED) is an additive manufacturing (AM) technique that uses metallic wire as the feedstock material. It could be broadly classified based on the utilised energy source, Fig. 1.3. Here, the focused energy source, such as a laser beam, electron beam, or arc, melts the fed wire and is continuously deposited onto a substrate or build platform. Once a layer solidifies the process continues to construct the desired three-dimensional component layer by layer. WF-DED is highly efficient for producing large-scale components, performing repairs, and conducting cladding applications due to its high deposition rates and minimal material waste, making it a more economical approach compared to powder-based technologies.

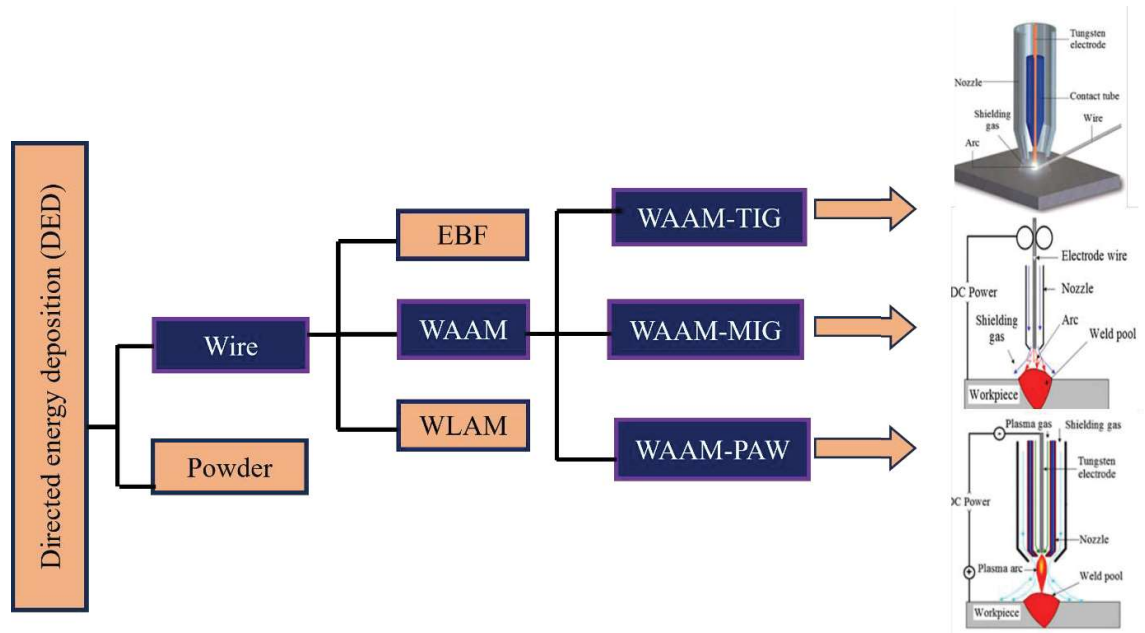


Fig. 1.3: Classification of directed energy deposition (DED) processes.[5]

### 1.2.2 Wire arc additive manufacturing (WAAM-TIG)

Wire arc additive manufacturing utilises tungsten inert gas (WAAM-TIG) as a heat source is a metal additive manufacturing process. It employs a non-consumable tungsten electrode and continuous feed of wire for its melting and deposition when fed into the stabilised TIG arc. WAAM-TIG is known for its superior control of input parameters, resulting in high-quality metal parts with refined microstructures and minimal residual stresses. This method is particularly suitable for processing reactive metals such as titanium, aluminium and others, due to its stable arc and low contamination risk. Despite its advantages, WAAM-TIG has limitations, including relatively slow deposition rates and the need for precise parameter control to prevent defects such as porosity and oxidation. Recent advancements focus on real-time monitoring, adaptive control, and multi-material deposition to enhance the efficiency and versatility of WAAM-TIG for industrial applications.

### 1.2.3 Wire Arc Additive Manufacturing (WAAM-MIG)

Wire arc additive manufacturing utilises metal inert gas (WAAM-MIG) as a heat source. It uses a consumable wire electrode fed coaxially for its melting and deposition of material layer by layer. This coaxial feeding of wire offers more

control of the deposition process than WAAM-TIG, making it more suitable for large-scale component fabrication. WAAM-MIG is widely used for materials such as steel, aluminium, and nickel-based alloys due to its efficiency and cost-effectiveness. However, challenges such as excessive heat input, spattering, and uneven bead geometry can impact the quality of the final part. To overcome these issues, researchers are integrating advanced control systems, pulsed MIG techniques, and real-time monitoring to improve bead uniformity and minimise thermal distortions. The growing application of WAAM-MIG in industries such as aerospace, automotive, and heavy machinery highlights its potential for producing complex, large-scale metallic structures.

#### **1.2.4 Wire Laser Additive Manufacturing (WLAM)**

Wire laser additive manufacturing (WLAM) utilises a high-power laser beam as a heat source and feed of wire feedstock externally similar to the WAAM-TIG. Since the process utilises a concentrated energy source of the laser, it ensures controlled melting and minimal heat-affected zones, which results in superior surface finish and mechanical properties compared to arc-based technologies. WLAM is particularly advantageous for applications requiring high accuracy and minimal material wastage, such as aerospace and biomedical industries. However, challenges include the high cost of laser systems, stringent process control requirements, and the need for advanced sensing technologies to maintain deposition accuracy. Ongoing research focuses on optimising laser power, wire feed rates, and closed-loop feedback systems to enhance process stability and material compatibility. WLAM's ability to produce complex geometries with high precision makes it a promising technology for next-generation metal additive manufacturing.

#### **1.2.5 Other wire -based systems**

Beyond WAAM-TIG, WAAM-MIG, and WLAM, other notable methods include wire electron beam additive manufacturing (WEBAM), which operates in a vacuum for deep penetration and high efficiency, making it ideal for aerospace and nuclear applications. Plasma arc wire deposition (PAWAM) provides higher energy density, improving deposition quality for materials like titanium. Wire induction additive



manufacturing (WIAM) uses electromagnetic induction for efficient, contactless heating, benefiting electrical and structural applications. Cold metal transfer (CMT) wire deposition minimises heat input, reducing distortions and making it suitable for automotive and lightweight aerospace components. Additionally, Hybrid Wire-DED, which combines arc and laser heating, enhances deposition speed and precision. Each process offers trade-offs in deposition rate, heat input, and control, with selection depending on factors like material type, part geometry, and application-specific requirements.

### **1.3 Review of pertinent literature in in-situ monitoring and feedback control system**

Numerous studies have demonstrated that real-time monitoring of power consumption, alongside variations in voltage and current, can serve as a reliable indicator of deposition quality. Researchers have explored additional input parameters such as deposition speed, wire feed speed (WFS), and associated output parameters, including temperature, acoustic emissions, and spectral radiation analysis to better understand and optimise the process. These investigations highlight the importance of process control in ensuring consistent deposition quality and mitigating defects that arise from uncontrolled parameter variations.

The traditional WAAM process predominantly relies on open-loop control systems, which lack the capability to adapt in real-time to fluctuations in process parameters. This limitation often leads to thermal inconsistencies, resulting in uncontrolled bead formation, variations in fusion depth, and defects that degrade the final component quality. Therefore, the incorporation of feedback-based control mechanisms has emerged as a promising approach to stabilise process parameters in real time, ensuring superior deposition quality and enhanced consistency [6], [7].

A comprehensive review by Kumar et al. (2022) summarised various analytical approaches, sensor technologies, and control strategies employed by different researchers to improve the quality of WAAM-produced components [8]. Similarly, Lebar et al. (2012) demonstrated that real-time voltage and current acquisition could

be effectively implemented using an isolation amplifier coupled with a voltage divider for voltage sensing and a Hall-effect sensor for current measurement (Fig 1.4). Their study, focused on metal inert gas (MIG) welding, established that fluctuations in voltage and current significantly influence the bead geometry, reinforcing the need for precise control in WAAM applications[8], [9].

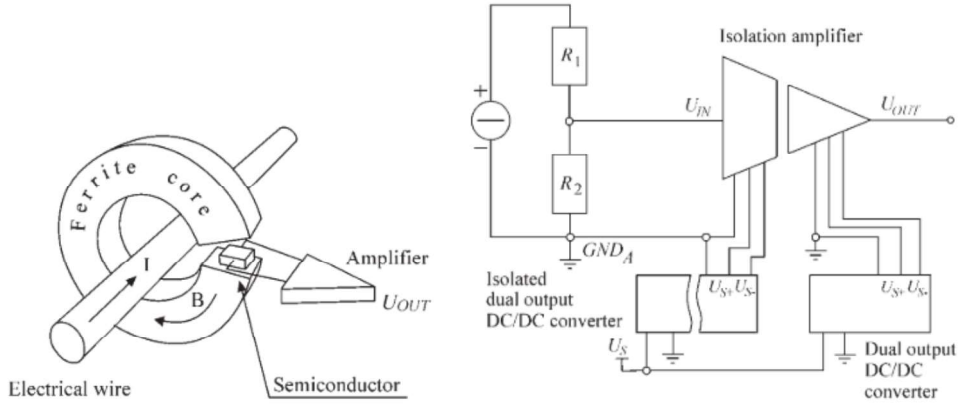


Fig. 1.4: (a) hall effect sensor (b) electronic circuit for voltage modification [9]

In efforts to regulate deposition quality, researchers have also explored feedback-based control of wire feed speed (WFS). Xia et al. (2022) utilised a CCD camera for melt pool monitoring, implementing a model predictive control (MPC) framework to real time adjust bead width. Their findings revealed that WFS has a direct correlation with bead width, which can be effectively controlled through adaptive regulation [10]. Additionally, studies have shown that WFS and deposition speed jointly influence bead geometry, where an increase in WFS enhances bead height, whereas a higher deposition speed reduces bead width due to rapid material deposition and constrained spreading. A PID-based feedback control mechanism has also been employed to regulate deposition speed and weld penetration depth [11]. Kejie et al. (2010) demonstrated that a controlled welding speed in gas tungsten arc welding (GTAW) significantly improves weld bead uniformity and penetration depth. Their work underscores the importance of real-time adaptive control in achieving optimal weld integrity and uniformity [12].

The interlayer temperature and dwell time between successive layers play a critical role in determining the bead geometry and overall structural integrity of the

deposited material. Various studies have explored the importance of maintaining a controlled thermal profile to enhance deposition quality and improve mechanical properties. Baier et al. (2022) utilised in-situ thermal imaging to actively monitor interlayer temperature and dwell times, ensuring a reproducible and uniform wall geometry [13]. Their research highlighted that maintaining an optimal interlayer temperature around 300°C resulted in greater stability of the fabricated component. By carefully regulating thermal fluctuations, they were able to minimise distortions and inconsistencies, demonstrating the significance of real-time temperature management in achieving uniform bead formation. Similarly, Wang et al. (2021) developed a structured control and monitoring system focused on regulating layer width. They implemented a closed-loop, collaborative control strategy that adjusted the welding current to ensure that the width and reinforcement of the weld bead met the desired specifications. Their experimental findings confirmed that real-time modifications to the molten pool width and reinforcement levels significantly improved deposition reliability. This study provided valuable insights into how adaptive control strategies can refine bead geometry and reinforcement-controlled reliability [14]. Jorge et al. (2022) assessed the suitability and limitations of employing infrared pyrometry to measure interlayer temperature in WAAM-MIG (Fig 1.5). Their research suggested that both open-loop and closed-loop control techniques could be explored to preserve the geometric and metallurgical integrity of the wall throughout the deposition process. This underscores the importance of precise thermal control in mitigating defects such as irregular bead formation, residual stresses, and material inconsistencies [15].

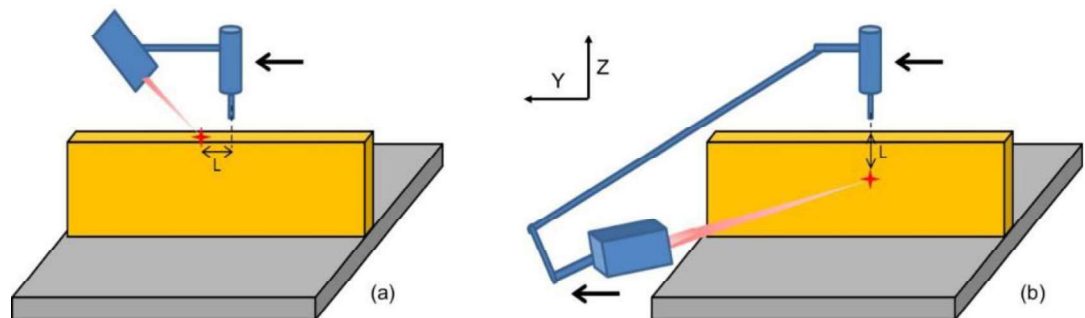


Fig. 1.5: Strategies for interlayer temperature measurement in thin wall WAAM: (a) Upper pyrometer strategy; and (b) sideward Pyrometer strategy [15]

In summary, the thermal behaviour of the deposition process plays a critical role in shaping the characteristics of the deposited bead. It directly affects deposition quality, material microstructure, residual stresses, and overall structural integrity. Effective temperature management is essential to achieving optimal cooling rates, which in turn influence grain refinement and phase transformations, leading to improved mechanical and metallurgical properties. Furthermore, maintaining a stable thermal profile minimises thermal distortions, enhances dimensional accuracy, and reduces the likelihood of defects such as porosity and cracks, ensuring superior build quality and structural reliability [16 - 19].

In recent years, Khan et al. (2022) introduced a real-time feedback-based control system for monitoring and regulating deposition temperature. Their study demonstrated that actively controlling temperature could alter bead geometry and mechanical properties in a controlled manner. By employing a two-colour ratio pyrometer, they accurately measured deposition temperature and implemented a PID-based feedback control system for single-layer bead deposition. This marked an important step towards integrating closed-loop thermal management into WAAM processes [20].

However, WAAM typically involves multilayer bead deposition, where thermal inconsistencies tend to accumulate as the number of layers increases. The present study builds upon this concept, extending its applicability to multilayer fabrication. By implementing real-time monitoring of electrical current and voltage, a more comprehensive integrated feedback system was developed to ensure consistent bead quality across multiple layers.

## **1.4 Objective and scope of the thesis**

The concept of Industry 4.0 was proposed for the fourth industrial revolution, which integrates automation, cloud computing, big data, and the internet of things (IoT) into modern manufacturing industries. This thesis aims to enhance both the automation level and intelligence of the WAAM-TIG process.

The primary objective of this research is to analyse the inconsistent thermal behaviour of deposited beads as the number of layers increases in the WAAM-TIG process. Real-time monitoring of electrical current and voltage has been integrated into the system to study their immediate impact on bead quality. By capturing and analysing these process parameters, the study aims to understand how fluctuations in thermal conditions affect deposition consistency, material integrity, and overall process stability. Addressing these thermal inconsistencies is crucial for improving the reliability and repeatability of multi-layered additive manufacturing.

To achieve this, a feedback control system has been developed to maintain a constant setpoint temperature during deposition. This ensures stable heat input, minimising defects such as overheating, excessive dilution, and irregular bead geometry. Furthermore, the study evaluates process efficiency by comparing the feedback-controlled system with a conventional open-loop system. Key performance indicators, including bead geometrical stability (width and height), specific energy consumption, hardness, and mechanical strength, are assessed to quantify improvements. The findings from this research will contribute to the development of more efficient, precise, and energy-optimised WAAM-TIG processes for industrial applications.

## **1.5 Thesis outline**

This thesis organisation is as follows:

Chapter 1, “Introduction” gives an overview of additive manufacturing fundamentals, key requirements, techniques, key literature on wire-fed DED (WF-DED), focusing on metal AM, and arc-based heat sources. It outlines research objectives for enhancing the WAAM-TIG process and provides a structured thesis outline.

Chapter 2, Outlines the "Experimental Setups and Instrumentation" utilised in this thesis research.

Chapter 3 gives an overview of In-situ voltage–current–temperature monitoring during WAAM-TIG for single and multi-layer deposition.

Chapter 4, Focuses on “Implementation of temperature dependent feedback control system to improve the process efficiency of WAAM-TIG” to regulate the properties of the deposited bead. Comprehensive experiments and validations are provided to demonstrate the concept and its practical application.

Chapter 5 provides a holistic “Conclusion” to the entire work.

## **Chapter 2**

### **Experimental setups and instrumentation**

#### **2.1 Introduction**

The experimental studies involved the use of various machines, instruments, and advanced techniques to explore different phenomena. This chapter provides an in-depth description of the key tools and methods employed throughout the research. It includes a thorough overview of the experimental setups, equipment, characterisation techniques, and data acquisition procedures utilised during the investigations. Detailed descriptions of specific experiments and methodologies are presented within their respective chapters.

#### **2.2 WAAM- TIG setup**

Fig. 2.1 illustrates the schematic representation of the WAAM-TIG system, highlighting its key components and their functions. The system is equipped with a TIG power source (Migatron PI-350 AC/DC), which provides a stable and controllable arc for precise heat input. The wire feeder (Migatron) is responsible for delivering the filler wire independently, with a maximum wire feed speed of 5 m/min, ensuring consistent material deposition during the process [21].

The WAAM-TIG system is automated using a CNC gantry and a Mach3 controller, ensuring precise torch and wire feeder movement along the programmed toolpath for accurate layer-by-layer deposition. The inert gas shielding system prevents oxidation, maintaining material quality, while real-time monitoring sensors track voltage, current, and temperature to detect anomalies such as heat accumulation and deposition inconsistencies. These integrated features enhance process efficiency, stability, and reliability, making WAAM-TIG ideal for fabricating high-quality metal components with complex geometries.

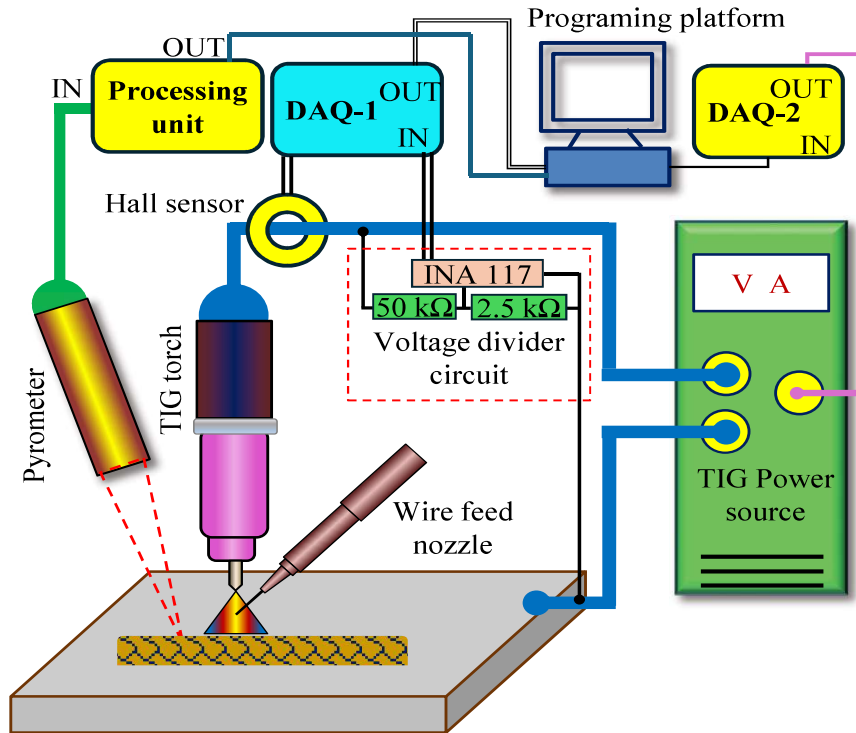


Fig. 2.1: Schematic of WAAM-TIG system with installed different modules for in-situ monitoring of voltage, current and temperature.

### 2.2.1 Current measurement

To measure the current in the WAAM-TIG process, a Hall-effect current sensor (LA305-S, measuring range  $\pm 500$  A) is employed (Fig.2.1, 2.2). This sensor is chosen due to its high sensitivity, non-intrusive measurement capability, and ability to detect both AC and DC currents accurately. The Hall-effect sensor operates on the principle of measuring the magnetic field generated by the flow of current through a conductor. The sensor is strategically positioned in the power circuit to capture real-time current variations during the deposition process. The sensor's output is an analogue signal that is conditioned and transmitted to a Data Acquisition (DAQ) system, which then processes and records the data using LabVIEW software. This setup enables continuous monitoring of current fluctuations.





Fig. 2.2: Hall effect sensor-LA305-S

### 2.2.2 Temperature measurement

Temperature measurements during the study were performed using a non-contact two-colour ratio pyrometer (LumaSense Technologies, IGAR-6 Advanced) (Fig. 2.3). The device operates at wavelengths of 1500–1600 nm and 2100–2500 nm for channel-1 and channel-2, respectively. It can also function in single-channel mode, considering radiation across the entire spectrum of both channels. The pyrometer features a minimum response time of 2 ms and a temperature measurement range of 250 °C to 2000 °C in ratio mode, and 100 °C to 2000 °C in single-channel mode.



Fig. 2.3: Pyrometer- IGAR-6

To ensure precise targeting, the pyrometer is equipped with a visible laser sight, enabling focus on objects with a minimum spot diameter of 2.1 mm. In order to measure the temperature during the deposition and further for the in-situ control, the pyrometer was focused at 12 mm behind the main melt pool. It was done to

avoid interference of arc and electrode radiation on temperature measurement. Monitoring at this offset provided a more stable signal for effective feedback control during the deposition. Further, the pyrometer was set to move along with the deposition head. It helps to capture the temperature profile along the deposition length rather than performing the measurement at a single point. Real-time temperature data can be monitored and recorded using the provided InfraWin software. Additionally, the pyrometer supports communication via ASCII codes (as outlined in the IMPAC Pyrometers IGAR-6 Advanced manual, 2019), making it particularly compatible with the LabVIEW platform for temperature control applications [20].

### **2.2.3 Voltage measurement**

Voltage measurement in the WAAM-TIG process is achieved using a voltage divider circuit in combination with an operational amplifier (INA-117) (Fig.2.1). The voltage divider circuit is designed to scale down the high voltage across the TIG electrode and the workpiece to a measurable range. The INA-117 operational amplifier ensures accurate signal conditioning by minimising noise and providing electrical isolation. The processed voltage signal is then fed into a Data Acquisition (DAQ) system, which records real-time voltage variations. This setup allows continuous monitoring of voltage stability, detecting fluctuations that may indicate arc instability, improper shielding gas flow, or electrode wear.

## **2.3 Materials**

For the experimental work, feed materials included Low Alloy Steel (ER70S-6, density 7850 kg/m<sup>3</sup>) with a diameter of 0.8 mm. AISI 1020 low-carbon steel plate measuring 300 × 150 × 5 mm<sup>3</sup> was primarily utilised as the substrate material in all experiments, unless specified otherwise. The chemical compositions of these materials are provided in Table 1.

**Table 1.1** Chemical composition of substrate plates and filler wire (ER70S-6) [22]

Element	C	Mn	P	S	Si	Cr	Ni	Mo	V	Cu	Fe
Mild steel	0.170-	0.3-	≤0.04	≤0.05	0.3-	-	-	-	-	-	99.08-
(AISI 1020)	0.230	0.6			0.6						99.53
ER70S-6	0.09	1.6	0.007	0.007	0.9	0.05	0.05	0.05	0.05	0.2	Bal

The WAAM-TIG process utilised argon gas as the shielding medium to prevent oxidation and ensure a stable arc environment, with a controlled flow rate of 10 L/min. Preliminary studies determined that an optimal combination of 130 A welding current, 2.5 m/min wire feed speed, and 150 mm/min deposition speed facilitated continuous and smooth material deposition.

## 2.4 Material characterisation

### 2.4.1 Sample preparation

Fig. 2.4 shows the schematic of sample locations for various analyses in a multilayer deposited wall. To examine the geometrical, hardness, and microstructural analysis, samples were extracted across the full build height of the bead. For strength analysis, specimens were cut in the build direction as per ASTM E8 [23] standards presented schematically in the subset of Fig. 2.4. All the samples were sectioned across the cross-section using a wire electro-discharge machining (EDM) system (CONCORD Wire EDM, DK7732). The specimens were then processed following standard metallographic techniques to ensure accurate material characterisation. Special precautions were taken to minimise excessive heat generation, preventing potential damage to the samples.

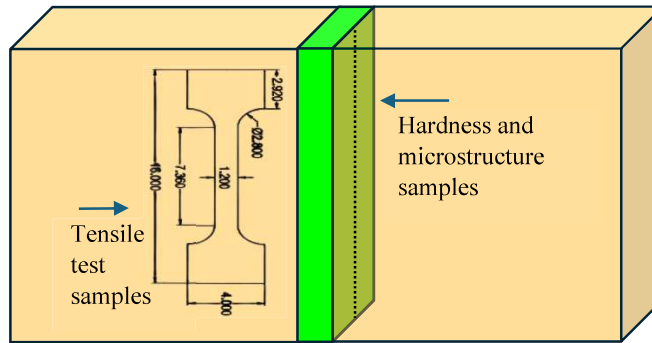


Fig. 2.4: Schematic of sample locations for various analyses in a multilayer deposited wall.

Sample preparation, adhering to established metallographic procedures, is crucial for material characterisation. This process involves a sequence of steps to ensure precise material analysis. The observation surface underwent polishing using abrasive papers, ranging from coarse ( $\sim 80$ ) to fine ( $\sim 2000$ ), followed by diamond abrasive polishing to achieve a mirror-like finish and reduce imperfections.

To reveal the microstructure, chemical etching was applied to low alloy steel using Nital solution for 5 seconds. These etching processes allowed for the visualisation of grain structure. Metallographic analysis provided valuable insights into grain size, phase structures, and other material properties, facilitating detailed examination and comparison of different material behaviours.

### 2.4.2 Geometry analysis

The geometrical accuracy of the deposited layers was assessed using laser displacement sensors (Micro-Epsilon opto-NCDT 1420) to measure the bead width, height, and layer uniformity. The analysis aimed to evaluate the impact of process parameters on the dimensional stability of the deposited structure. The study revealed that the implementation of a feedback-controlled system resulted in a more uniform bead profile, reducing deviations in width and improving height consistency.

### 2.4.3 Optical Microscopy

Microstructure of cross section was observed using optical microscope (BX53M Olympus) along the build direction.



Fig. 2.5: optical microscope setup

### 2.4.4 Micro-Indentation Hardness

Micro-indentation hardness testing was performed using Vickers hardness test to evaluate the hardness distribution along the build direction, where a square-based pyramidal diamond indenter with specified face angles is pressed into the material under controlled conditions. After applying and removing the test force, the diagonal lengths of the indentation are measured to determine the Vickers hardness number (HV). This number is calculated as the applied test force  $F$  (kgf) divided by the surface area (AS) of the indentation ( $\text{mm}^2$ ), as expressed by:

$$HV = \frac{F(kgf)}{AS(\text{mm}^2)}$$

The surface area (AS) is derived using the formula:

$$AS = \frac{d^2}{1.8544}$$

where  $d$  represents the average diagonal length of the indentation.



Fig. 2.6: Vicker hardness tester setup

For this study, a Mitutoyo HM-210 Type A or UHL VMHT Vickers hardness tester was used. A 300kgf load was applied for a total duration of 18 seconds, which included a loading time of 4 seconds, a hold time of 10 seconds, and an unloading time of 4 seconds. Hardness values were measured along a vertical line at the centre of the deposited beads or multilayer structure, and the average values were taken for comparative analysis.

### 2.4.5 Strength Analysis

The tensile strength of the deposited samples was analysed using ASTM-E8 [23] standard tensile testing procedures with a Shimadzu AGX-V universal testing machine at a crosshead speed of 1 mm/min.



Fig. 2.7: UTM setup for tensile test.

## **Chapter 3- In-situ voltage–current–temperature monitoring during WAAM-TIG**

### **3.1 Introduction**

Wire arc additive manufacturing utilising tungsten inert gas (WAAM-TIG) as heat source is a widely used technique for fabricating metallic components due to its flexibility, cost-effectiveness, and capability to build large-scale structures. Among the key parameters influencing the deposition process, voltage, current, and temperature play a crucial role in determining bead geometry, layer bonding, and overall part integrity. Any fluctuations in these parameters can lead to process instability, defects, and inconsistencies in material properties.

Traditional WAAM systems often operate in open-loop mode, where there is no real-time adjustment of these process parameters, leading to varying thermal profiles, distortions, and suboptimal material utilisation. However, the introduction of an in-situ monitoring system allows for the continuous monitoring and regulation of voltage, current, and temperature during deposition. This real-time data acquisition and analysis provide valuable insights into the process behaviour, enabling adaptive control strategies to optimise deposition quality and efficiency.

In this section, in-situ monitoring of voltage, current, and temperature (C-V-T) is investigated for both single-layer and multi-layer depositions. The aim is to analyse the effect of process conditions dynamics on bead formation, interlayer bonding, and component stability. The findings from this study highlight the significance of real-time monitoring in improving process efficiency, minimising defects, and ensuring consistent deposition in WAAM-TIG applications.

### **3.2 In-situ C-V-T monitoring during single-layer deposition**

Fig 3.1 presents the recorded profiles of current, voltage, and temperature during the deposition of a single-layer bead. The data acquisition system effectively captured all these parameters with high precision and minimal signal interference. Notably, repeated experiments demonstrated consistent parameter values, indicating reliable system performance. The deposition was performed for a length of 100 mm for both single and multilayer bead deposition.

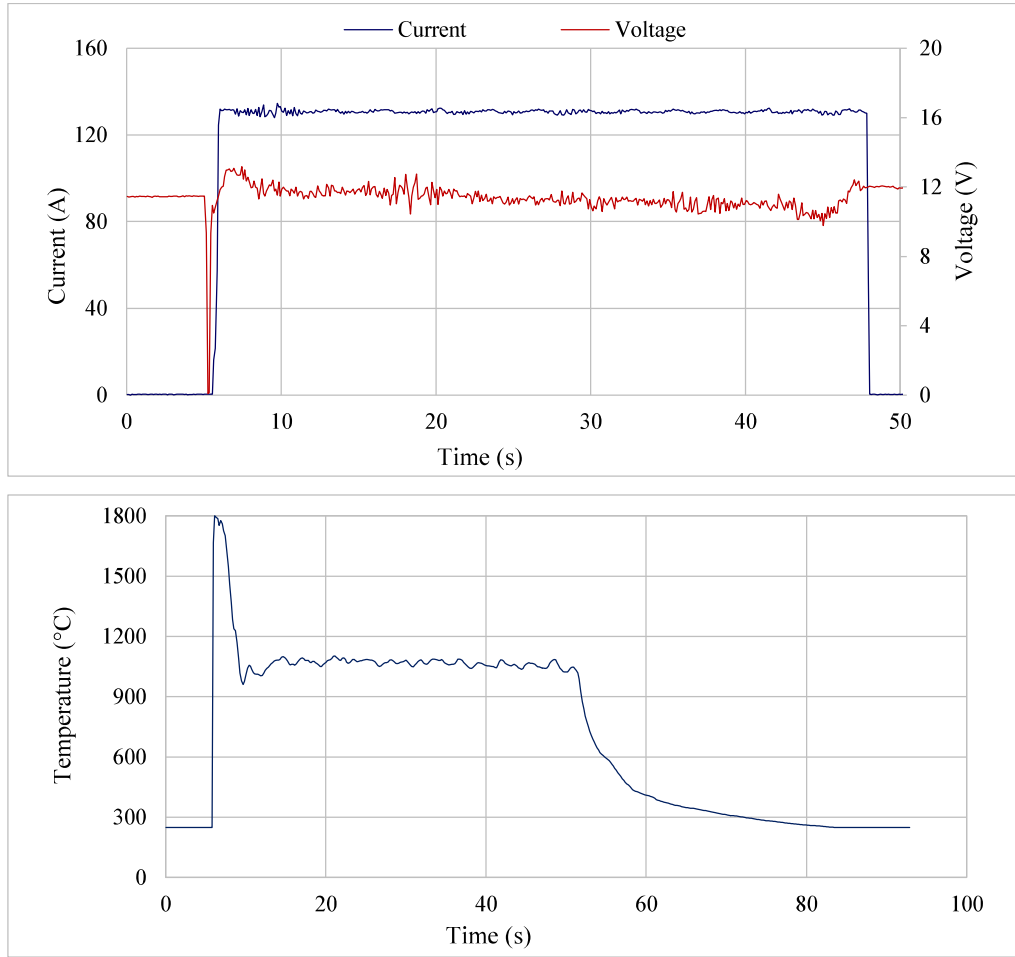


Fig. 3.1: The recorded (a) voltage and current, and (b) temperature profile for single-layer bead deposition.

The stability of these parameters plays a crucial role in ensuring uniform arc behaviour, which is fundamental for process repeatability and quality control. A steady arc condition directly influences the thermal distribution, melt pool dynamics, and solidification characteristics, all of which are critical for maintaining uniform bead geometry. This consistency becomes even more significant when transitioning to multilayer deposition, where variations in arc stability can lead to defects such as irregular bead profiles, excessive heat accumulation, or lack of fusion between layers. The recorded data, therefore, serves as a strong foundation for further investigation into multi-pass and multi-layer deposition strategies, facilitating the development of a more robust and controlled WAAM-TIG process.



### 3.3 In-situ C-V-T monitoring during multi-layer wall deposition

Fig. 3.2 illustrates the recorded current, voltage, and temperature profiles observed during the deposition of a multilayer (10-layer) bead. The experimental data reveals that while the recorded current and voltage remain relatively stable and consistent across successive layers, the bead temperature exhibits a progressive increase as additional layers are deposited. This trend suggests that heat accumulates within the structure over time, influencing the overall thermal behaviour of the deposition process.

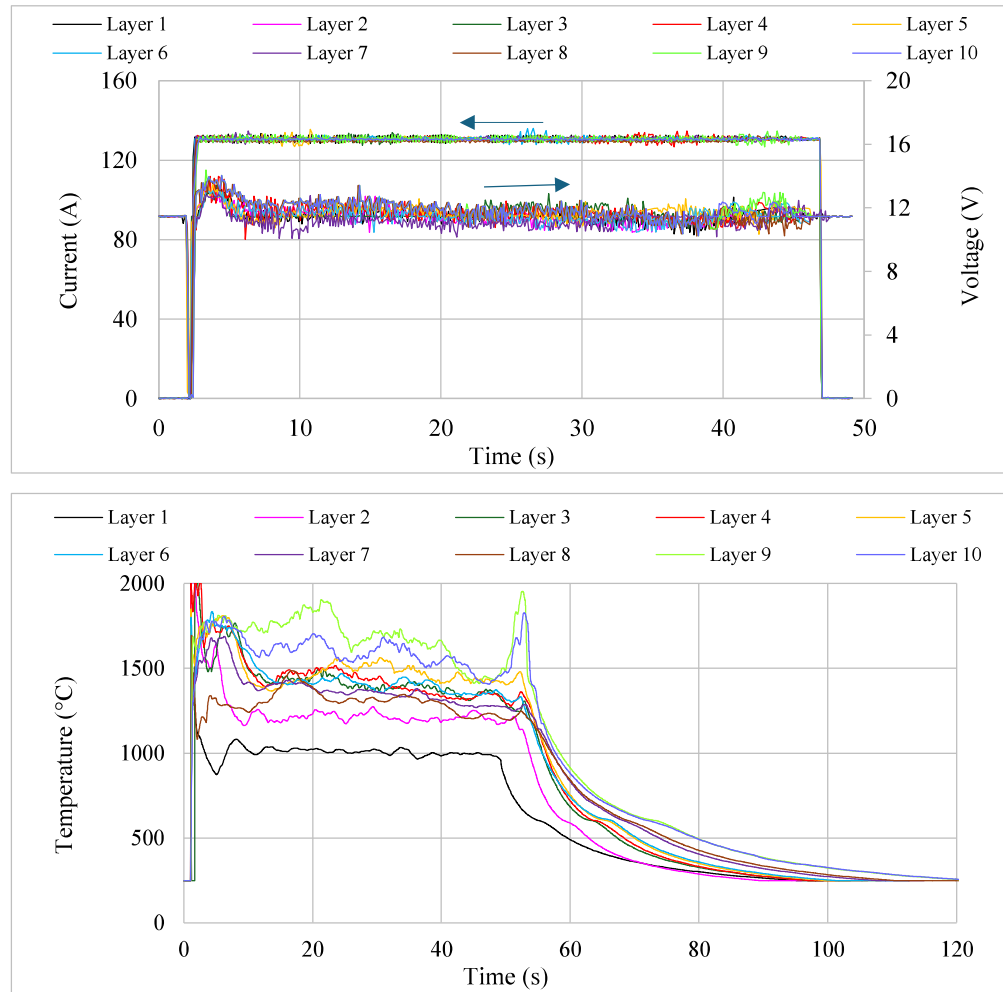


Fig. 3.2: The recorded (a) voltage and current, and (b) temperature profile for multilayer bead deposition.

Additionally, noticeable variations in temperature stability and cooling rates were observed with an increasing number of layers. These fluctuations indicate that the deposited material retains heat for extended periods, leading to prolonged thermal

exposure. As a result, continuous energy input without adequate heat dissipation can result in excessive heat buildup, increasing dwell time and the risk of overheating. This phenomenon is attributed to a shift in the dominant heat transfer mechanisms. In the initial layers, conduction plays a significant role in dissipating heat through the substrate and surrounding material. However, as the deposition progresses, conduction efficiency diminishes, and convection and radiation become the primary modes of heat transfer. This transition reduces the overall heat dissipation rate per unit time, creating a higher thermal gradient within the material. Consequently, the accumulation of heat contributes to a larger melt pool, enhanced fusion depth, and potential instability in bead geometry (Fig.3.3) [24].

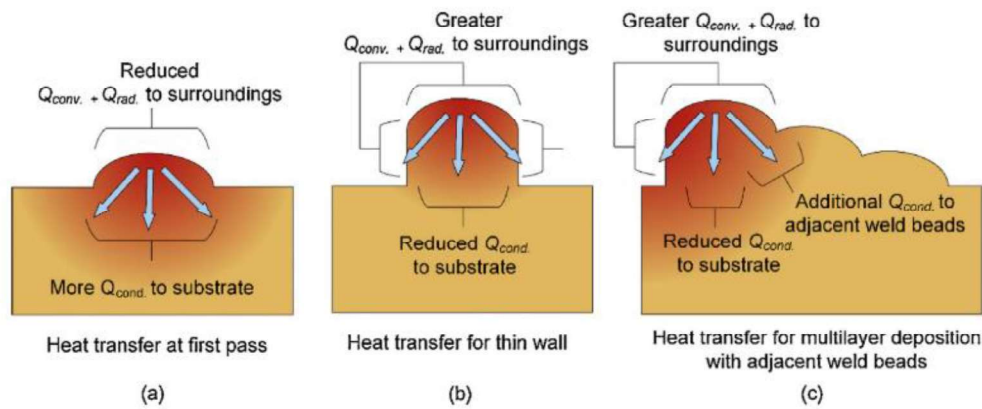


Fig. 3.3 Schematic diagram of the heat dissipation modes, conduction ( $Q_{cond}$ ), convection ( $Q_{conv}$ ), radiation ( $Q_{rad}$ ) [24]

The implications of this overheating are critical, particularly for multilayer wall deposition. Excessive heat retention can lead to deteriorating bead quality, causing an increased aspect ratio in previously deposited layers. This thermal imbalance may also compromise the structural integrity of the build, introducing defects such as warping, residual stress accumulation, and crack formation. These defects adversely impact the mechanical properties of the final component, reducing its reliability and performance in practical applications.

To address these challenges and ensure stable thermal conditions throughout the multilayer deposition process, a real-time feedback control system was developed. This system continuously monitors the bead temperature and real time adjusts the input energy to prevent excessive heat buildup. By actively regulating power based

on temperature fluctuations, the control mechanism enhances process stability, ensures uniform bead geometry, and minimise the risk of thermal-induced defects. This approach is essential for achieving high-quality, defect-free multilayer structures in WAAM-TIG, improving both mechanical integrity and overall process efficiency.

### **3.4 Results and discussion**

The real-time monitoring of voltage, current, and temperature during both single-layer and multi-layer WAAM-TIG deposition provided critical insights into process stability, thermal behaviour, and deposition quality.

In single-layer deposition, the recorded voltage and current profiles exhibited minimal fluctuations, ensuring a stable arc and uniform energy input, which contributed to controlled melt pool formation and consistent bead geometry. The temperature profile showed predictable heating and cooling cycles, with efficient heat dissipation through the substrate, preventing excessive thermal buildup.

However, in multi-layer deposition, while voltage and current remained stable, the recorded temperature demonstrated a continuous upward trend as layers accumulated, leading to increased heat retention and prolonged cooling times. This shift in heat transfer mechanisms, from conduction-dominated dissipation in initial layers to convection and radiation in later stages, resulted in larger melt pools, altered bead dimensions, and increased residual stress. The excessive thermal accumulation posed challenges such as geometric inconsistencies, warping, and potential degradation of mechanical properties. To address these issues, a real-time feedback control system was implemented, real time adjusting power input based on temperature fluctuations, effectively stabilising interlayer temperatures, minimising thermal defects, and ensuring repeatable, high-quality multi-layer deposition. These findings underscore the importance of precise thermal regulation in WAAM-TIG, demonstrating that adaptive control strategies are essential for maintaining process stability and achieving defect-free metallic structures.

## **Summary**

In-situ monitoring of voltage, current, and temperature in WAAM-TIG revealed stable behaviour of these signals for single-layer bead deposition leading to uniform bead geometry. However, with an increase in the number of layers, the temperature signals showed inconsistent behaviour. The possible reason could be the accumulation of heat in multi-layer deposition, which also affected the cooling rate, bead geometry and mechanical properties (included in Chapter - 4). Therefore, in order to minimise this heat accumulation, a real-time feedback control system is needed to regulate input energy and improve process stability.

## **Chapter 4**

### **Implementation of temperature dependent feedback control system to improve the process efficiency of WAAM-TIG**

#### **4.1 Introduction**

Wire arc additive manufacturing using tungsten inert gas (WAAM-TIG) is an advanced fabrication technique that requires precise control over process parameters to ensure consistent and high-quality deposition. However, one of the critical challenges associated with WAAM-TIG is maintaining a consistent thermal profile throughout the deposition process. Variations in temperature could lead to irregular bead geometry, microstructural inconsistencies, and mechanical properties. To address these, a temperature-dependent feedback control system has been developed and implemented in the WAAM-TIG process. This system continuously monitors the thermal behaviour of the deposition in real time and regulates the heat input to ensure uniform thermal conditions. Unlike conventional open-loop systems, which operate under fixed input parameters and fail to compensate for temperature fluctuations, the feedback-based approach enables precise energy regulation.

This chapter presents the development and implementation of the feedback control system, detailing its integration into the WAAM-TIG process. The effectiveness of the system is evaluated based on improvements in deposition quality, process repeatability, and efficiency. Key aspects such as the impact on bead geometry, material utilisation, and mechanical integrity are studied and discussed in detail. Through this study, the proposed control mechanism aims to establish a reliable WAAM-TIG process, paving the way for high-quality, and defect-free additive manufacturing of metallic components.

#### **4.2 Development and implementation of a PID-based feedback control system for WAAM-TIG**

A dedicated feedback-based control system was developed to regulate the input energy during the WAAM-TIG process, ensuring stable thermal conditions and mitigating overheating challenges associated with multilayer deposition. This

system incorporated a Proportional-Integral-Derivative (PID) controller, a widely used control mechanism for maintaining process stability through continuous monitoring and corrective adjustments. Since the TIG welding process operates on a constant current principle, the feedback control system was specifically designed to regulate input current, as it directly influences the energy supplied to the arc and, consequently, the heat input into the deposition process. The primary objective of this control strategy was to counteract the gradual temperature rise observed in multilayer deposition (as illustrated in Fig. 3.2), thereby preventing excessive heat accumulation and ensuring continuous and defect-free material deposition. The deposition was performed for a length of 180 mm for multilayer bead deposition.

Fig. 4.1 presents the workflow of the developed feedback control system, which integrates continuous monitoring with real-time energy regulation to maintain optimal deposition conditions. The process begins with the tungsten inert gas (TIG) Welding power source supplying the initial current required for the deposition. To enable seamless automation and control, the conventional foot pedal used for manual current adjustment in TIG welding was replaced with a data acquisition (DAQ) system.

This foot pedal regulates the reference DC voltage instead of the actual TIG parameter (current) available at the torch typically varying in the range of 0–10 V. The actual current available for welding/ WAAM was found proportional to this reference voltage where the ‘0 V’ represents the minimum and ‘10 V’ is the maximum set TIG current on the machine, respectively. On the physical foot pedal, with the application of the load, the potentiometer wiper position changes, which defines the resistance (0–10 k $\Omega$ ) and, hence, the reference voltage. Here, it was directly regulated by the analogue output of the DAQ system. It was done to facilitate the direct communication between the welding power source and implement the feedback control system [20].

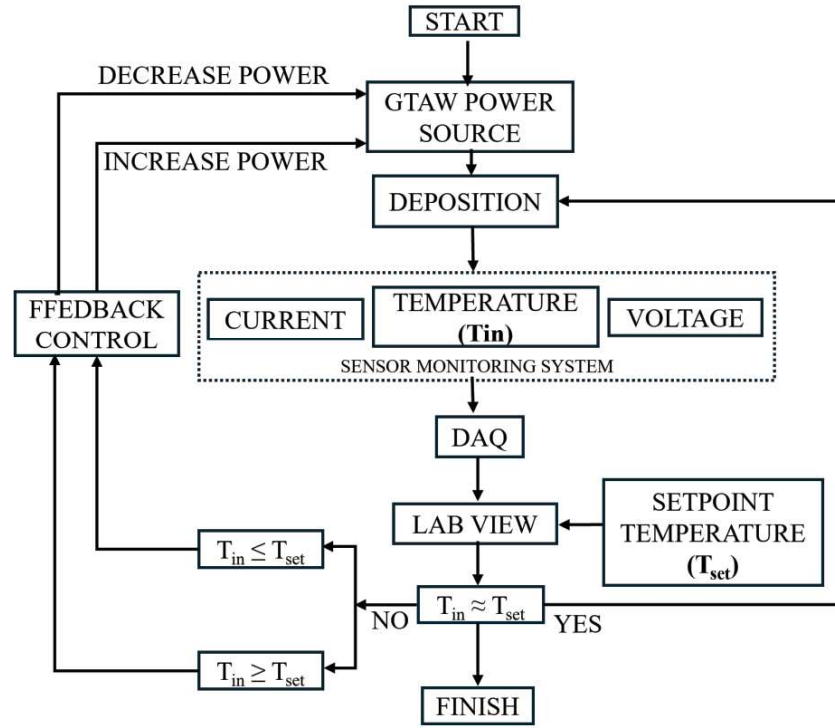


Fig. 4.1: Logical flow chart of the closed-loop feedback control system.

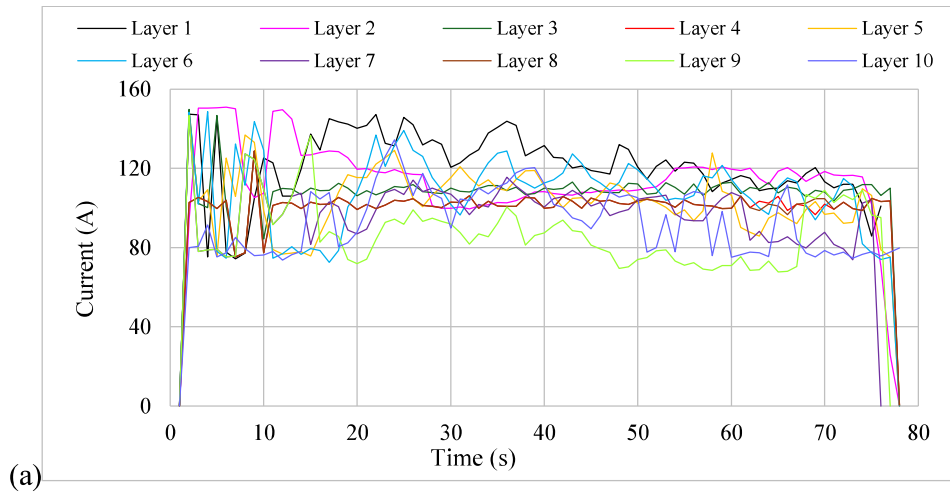
The control system was programmed in LabVIEW to interface with multiple sensing components, including a pyrometer for temperature measurement, a Hall effect sensor for current monitoring, and a voltage divider circuit for voltage measurement. These sensors continuously monitor the operational parameters in real-time and transmitted the data to the control system. The measured deposition temperature ( $T_{in}$ ) was continuously compared against a predefined setpoint temperature ( $T_{set}$ ), and depending on the response, the feedback system interacts with the power source to regulate the input energy in real time.

The effectiveness of the PID controller is heavily dependent on the appropriate selection of its constants, i.e. proportional gain ( $K_p$ ), integral gain ( $T_i$ ), and derivative gain ( $T_d$ ). In order to find the suitable range on these constants in WAAM-TIG, a series of pilot experiments were performed and found through iteration as follows,  $K_p=0.0478$ ,  $T_i=0.0023$ , and  $T_d=0.0330$ . These values were chosen to ensure a balanced response between stability and adaptability. Improper tuning of these parameters could lead to process instabilities, for example, an incorrect  $K_p$  value could cause either excessive heating or an excessively slow response, leading to

irregular bead formation. Similarly, suboptimal  $T_i$  or  $T_d$  values could introduce process lags or oscillations, adversely affecting deposition quality, bead uniformity, and overall mechanical integrity [22], [24].

The feedback controller continuously receives input data from the sensors, allowing it to make real-time adjustments to the input energy. This closed-loop control mechanism ensures that the WAAM process maintains the desired thermal conditions, thereby enhancing the quality and efficiency of the deposition. The process terminates once the temperature stabilises within the setpoint range, indicating successful control and completion of the deposition cycle.

Fig. 4.2a shows the recorded current and temperature behaviour with the developed close-loop feedback-based control system for the deposited 10-layer wall. Here, the setpoint temperature ( $T_{set}$ ) was kept constant at 1250 °C and the implemented PID controller was regulating the required input current. It was observed that the developed control system works efficiently for multilayer deposition and could maintain the desired set point temperature (Fig. 4.2b). Notably, the voltage remained consistent at ~ 12 V similar to an open loop system. However, the current was observed to diminish and later tends to stabilise with the increase in the number of layers (Fig. 4.1a).





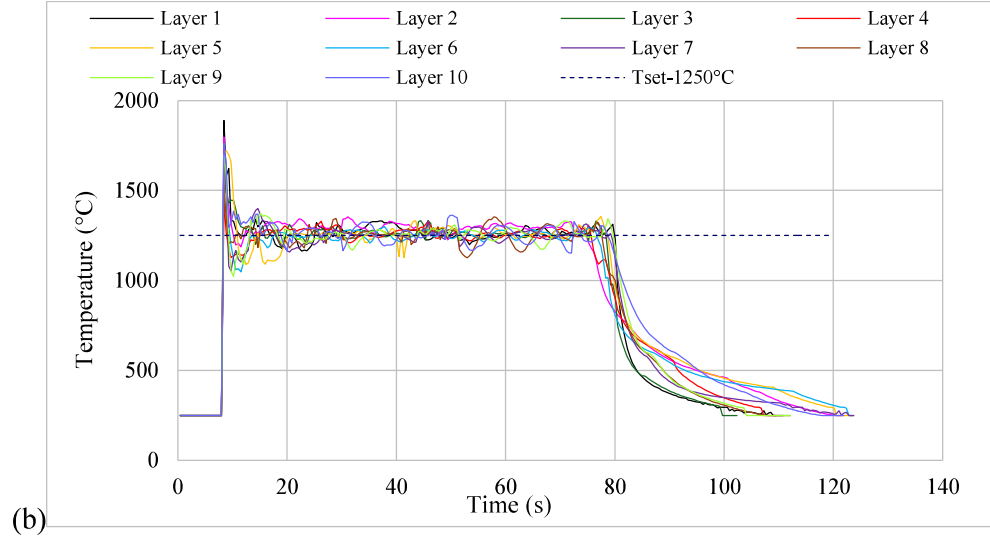


Fig. 4.2: The recorded (a) voltage and current, and (b) temperature profile for multilayer bead deposition with controller.

## 4.3 Results and discussion

### 4.3.1 Effect of feedback control system on process efficiency

The system effectively maintained the desired setpoint temperature throughout the deposition process, as depicted in Figure 4.2(b), ensuring a stable thermal environment and the current exhibited a noticeable trend. Initially, as additional layers were deposited, the input current gradually decreased before stabilising at a lower value (Fig. 4.2a). This behaviour is indicative of an adaptive energy management process. Therefore, the process efficiency of multilayer deposition in WAAM-TIG was studied for the developed closed-loop feedback control system.

$$\text{Specific Energy (J/mm}^3\text{)} = \frac{\text{Voltage} \times \text{Current}}{\frac{\pi}{4} \times d^2 \times \frac{wfs}{60}} \quad \dots E q. 1$$

The reduction in current had a profound impact on the specific energy consumption of the process. Specific energy, mathematically presented in Eq. 1, is defined as the amount of energy needed to melt a unit volume of the material (J/mm<sup>3</sup>). The average current utilised for the deposition of a layer was considered for the calculation. It was observed that the reduction in the current significantly decreased the specific energy requirements. The estimation of specific energy was based on the average current utilised per layer during deposition.

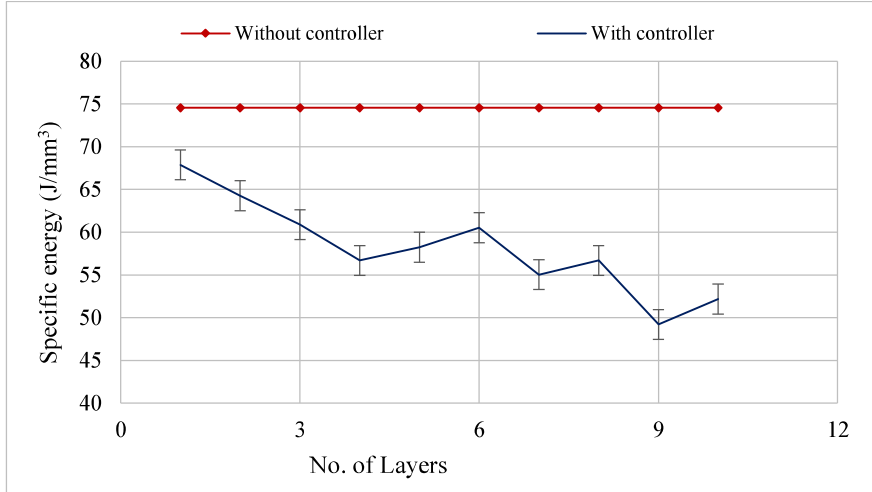


Fig. 4.3: The obtained specific energy with the number of layers, with and without a controller

It was found that the total energy consumption per unit volume of the material decreased significantly with the increase in the number of layers (Fig. 4.3). Overall, the implementation of the feedback control system led to a ~22% improvement in process efficiency compared to the conventional open-loop system. This improvement in energy efficiency directly translates into enhanced process sustainability and cost-effectiveness. By reducing unnecessary heat input, the feedback system not only optimised energy/material utilisation but also mitigated the risks associated with excessive heat accumulation, such as increased melt pool size, distortion, and residual stress development.

The ability to regulate input energy based on continuous temperature feedback not only conserves power but also ensures process stability, reliability, and repeatability. Such an intelligent control mechanism is crucial for industrial-scale WAAM-TIG applications, where precision, efficiency, and sustainability are critical to achieving high-quality additive manufacturing outcomes.

### 4.3.2 Effect of feedback controller on various properties

#### *Bead profile analysis*

The effect of the closed-loop feedback-based control system on bead geometry was thoroughly analysed and presented in Fig. 4.4. A laser displacement sensor (Micro-Epsilon opto-NCDT 1420) has been used to determine the profile geometry.

It was observed that the controlled deposition leads to more uniform wall deposition. The bead width decreased, and the height increased as compared to the without controlled multilayer wall deposition (Fig. 4.4a and b). The average wall width was found to decrease from  $\sim 7.2$  mm to  $\sim 6.14$  mm, whereas height was increased from  $\sim 13.7$  mm to  $\sim 17.42$  mm. So, for the controlled bead geometry profile, there is balanced deposition which is crucial for structural integrity, and it highlights the effective material deposition and process control. The results show the effectiveness of the control system in achieving more uniform bead geometry and optimum material utilisation by reducing excess spread or small melt pool size.

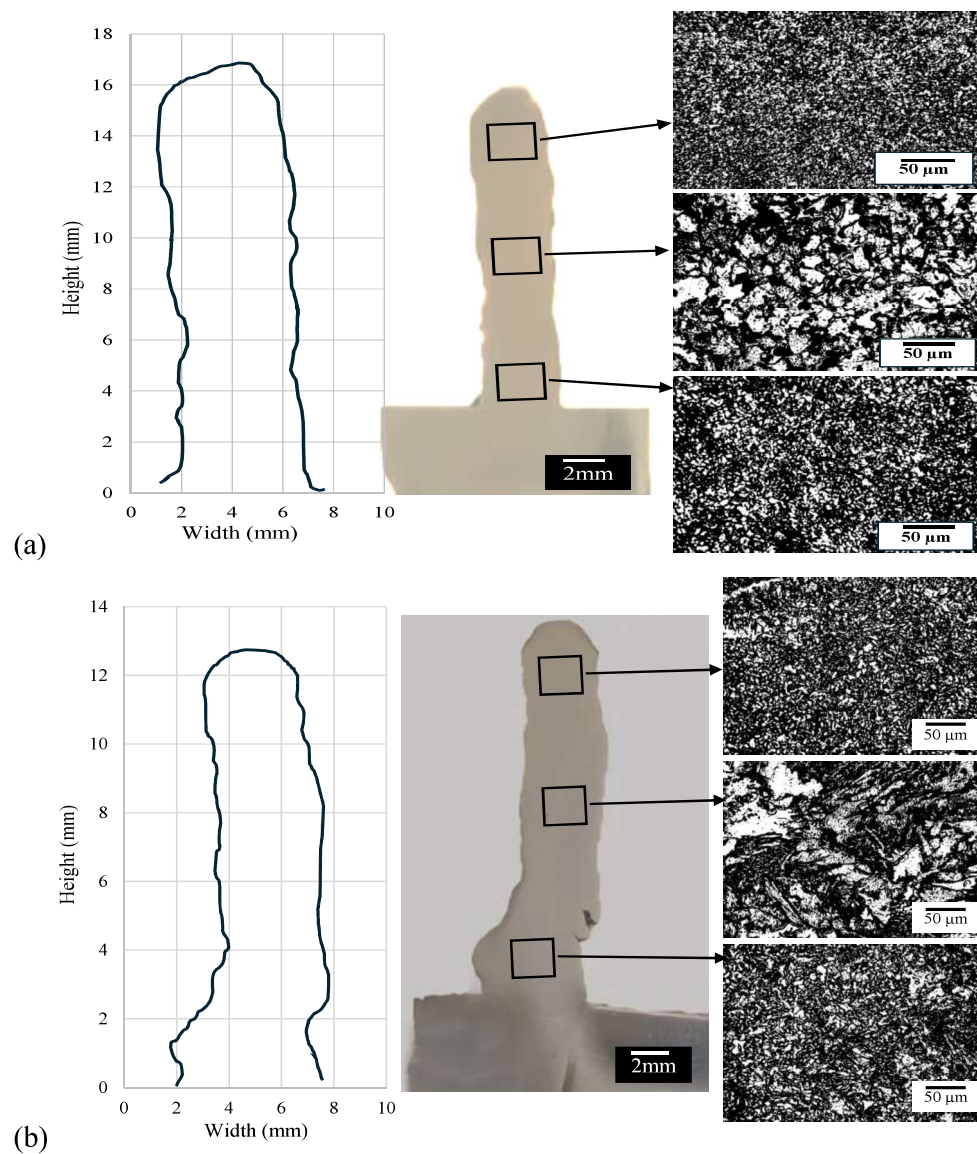


Fig. 4.4: The obtained bead profile for multilayer wall and microscopic images across wall height for (a) with and (b) without controlled deposition.

### *Hardness and microstructural analysis*

The micro-indentation hardness and microstructural analysis were performed (Mitutoyo HM-210 Type-A tester) to study any adverse effect of controlled temperature deposition on mechanical properties. Fig. 4.5a shows the obtained hardness along the height of the deposited wall. Little effect of controlled temperature deposition was observed on measured hardness. Figure 4.4a and b shows the obtained microstructure from the optical microscope (BX53M Olympus) along the build direction. Insignificant change was observed in microstructures irrespective of the mode of deposition i.e., with and without controller. In general, the overall trend was the formation of finer grains for the initial layers, coarser grains in the middle and again relatively finer grains at the upper regions of the wall.

In order to understand this hardness and microstructural behaviour, the cooling rate was determined from the temperature profile of each layer across the range of 1000 °C to 250 °C throughout the cooling cycle. Fig. 4.6a shows the typical temperature profile recorded during the deposition. It also depicts the identified temperature (points A' and C ) and cooling time. The mathematical equation to calculate the cooling rate is presented in Eq. 2. The cooling rate was found to gradually decrease with the increase in the number of layers presented in Fig. 4.6(b), following a natural trend [22]. However, in the case of controlled deposition, it was relatively more stable and marginally higher compared to without controlled deposition. This could be attributed to heat accumulation, which slows the cooling process, or heat dissipation. Comparatively, the controlled deposition effectively manages energy input, sufficient to melt the material only, preventing overheating and heat buildup. This ensures a stable cooling rate throughout the deposition process. This underscores the importance of thermal control systems in achieving consistent cooling during multi-layer deposition. The initial decreasing trend in hardness could be attributed to thermal gradients where the heat is dissipated into the substrate rapidly, resulting in higher cooling rates and a fine grains microstructure.

$$\text{Cooling rate} = \frac{1000\text{ }^{\circ}\text{C (A')} - \text{Reference minimum temperature, } 250^{\circ}\text{C,}}{\text{Cooling time (s)}}$$

...Eq. 2

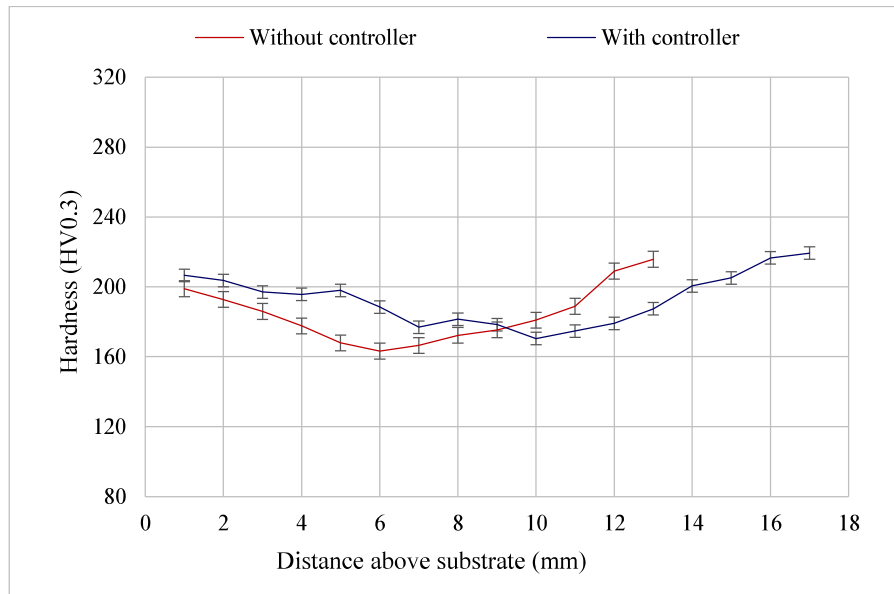
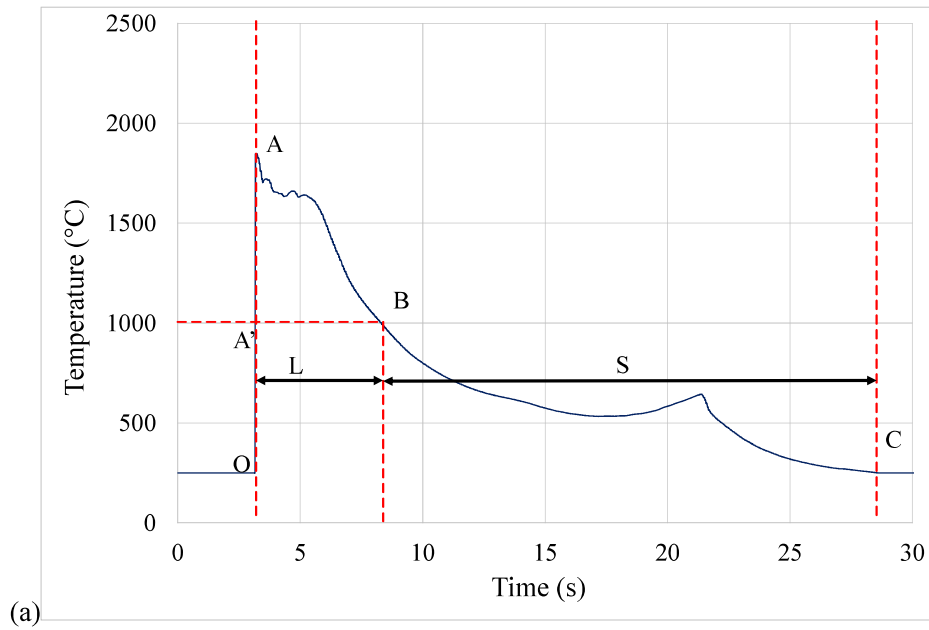


Fig. 4.5: The obtained hardness behaviour with and without a controlled deposition.



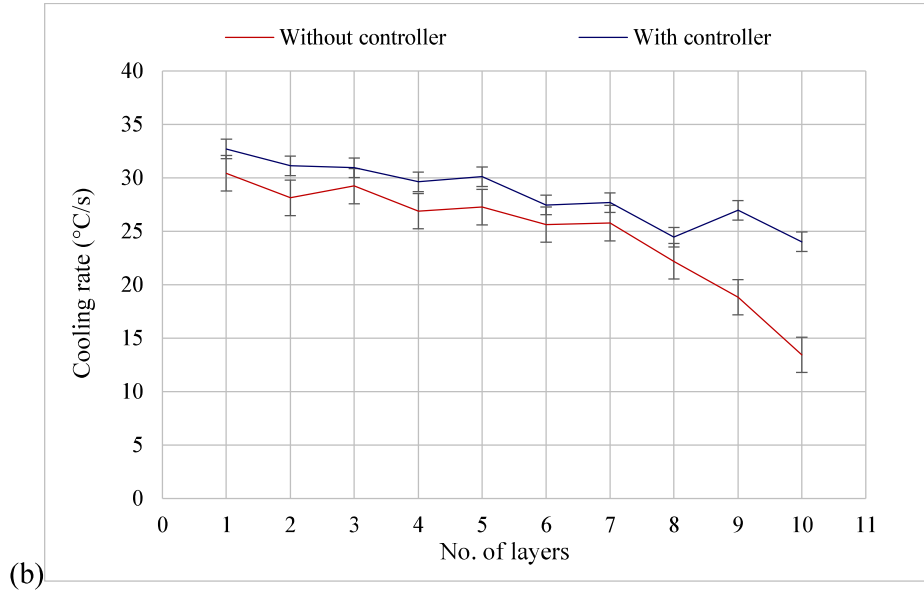


Fig. 4.6: The (a) typical temperature profile and calculation for cooling rate, and (b) the obtained cooling rate with and without a controlled deposition.

However, the intermediate layers bear multiple heating and cooling cycles due to layer-by-layer deposition leading to the coarsening of grains in these regions except for the top region [25]. The marginal decrease in hardness in the central area of the deposited wall may be attributed to the development of these coarser grains.

#### *Strength analysis*

The tensile test was also performed along the build direction to ensure good fusion between the layers with the proposed feedback-based controlled deposition. The procedure was performed on ASTM standard cut samples (E8) at a crosshead speed of 1 mm/min utilising universal testing equipment (Shimadzu AGX-V). The Fig. 4.7 shows the schematic and pictorial view of the test samples before and after the tensile test. The obtained stress-strain curve is presented in Fig. 4.8

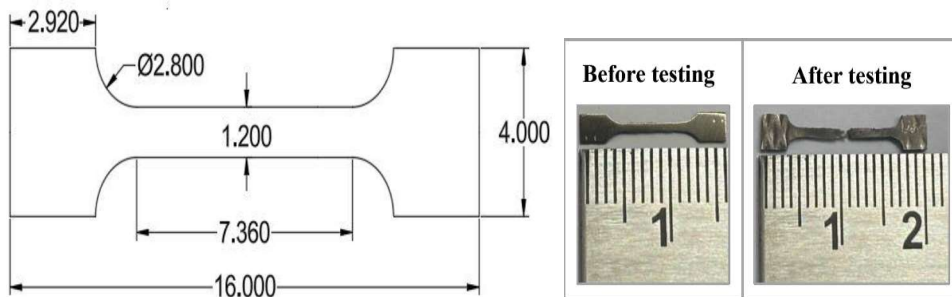


Fig. 4.7: The schematic and pictorial view of the test samples before and after the tensile test

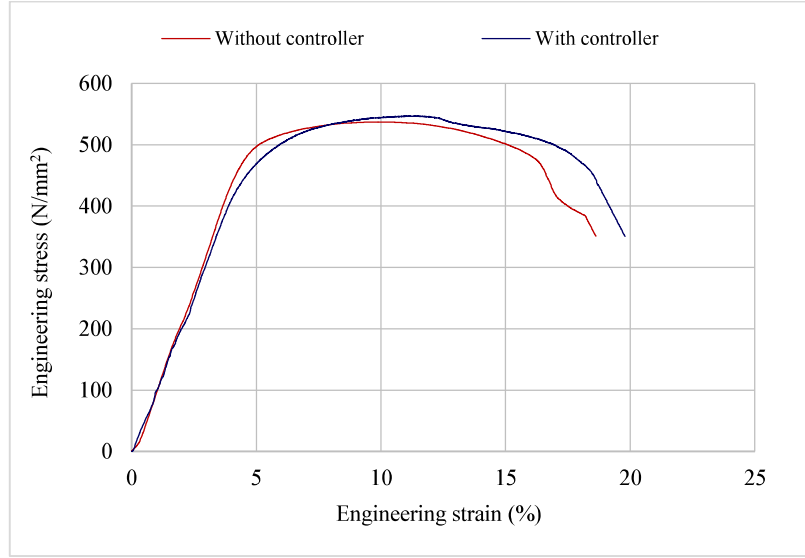


Fig. 4.8: The obtained stress-strain curve for multilayer deposited samples with and without a controller.

The obtained ultimate tensile strength (UTS), yield strength (YS) and % elongation values are presented in Table 4.1.

**Table 4.1.** The obtained UTS, YS and % elongation for, with and without the controlled deposition.

	<b>Yield strength (YS)</b>	<b>Ultimate tensile strength (UTS)</b>	<b>% elongation (<math>\epsilon</math>)</b>
<b>With controlled</b>	$427.8 \pm 17 \text{ N/mm}^2$	$546.7 \pm 21 \text{ N/mm}^2$	19.64%
<b>Without controlled</b>	$454.7 \pm 18 \text{ N/mm}^2$	$538.2 \pm 21 \text{ N/mm}^2$	18.53%

It could be seen that the excellent YS was obtained i.e. ~80% and ~85% of UTS in the case of with and without controlled deposition, respectively. Also, these values were found to be in similar ranges available in the literature for low alloy steel [26], [27]. In summary, it could be said that the successful implementation of the proposed system could be scaled up for industrial applications without compromising the mechanical properties. It offers significant benefits in terms of overall process efficiency, quality, and cost-effectiveness in additive manufacturing processes [28], [29]. An increase in wall height for the same material deposition rate

is another advantage of the process which makes it a perfect choice for the fabrication of thin-walled larger components.

#### 4.4 Scalability analysis

The proposed temperature dependent feedback based controlled system could lead to efficient deposition. In order to understand its effect on the fabricating of large-size components a scalability analysis was performed. Two geometries were considered for this analysis, schematically presented in Fig. 4.9.

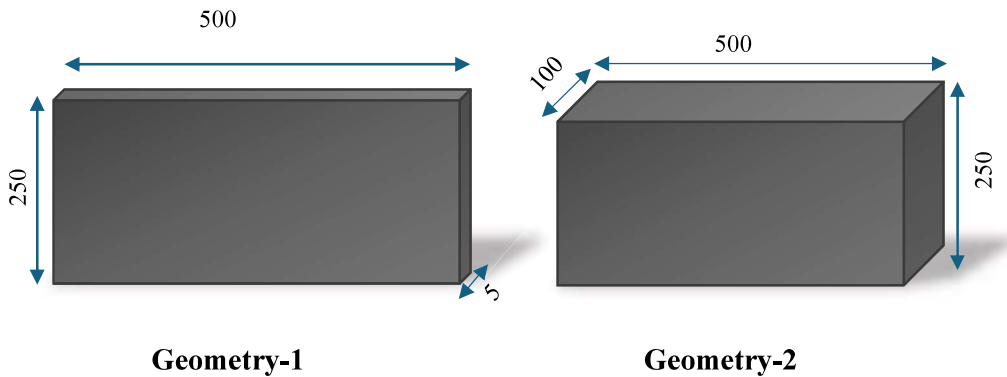


Fig. 4.9: Schematic diagram of geometry -1 and geometry-2 (dimension in mm)

In this analysis, a generally used  $\sim 40\%$  overlap between adjacent layers was considered [30], [31]. It was compared based on overall energy utilisation, number of layers, part build time and material utilisation, as presented in Table 4.1. Based on the conducted theoretical analysis, it could be concluded that the process with controlled temperature deposition has performed relatively better. Also, the fabricated parts are expected to be closer to the true geometry.



**Table 4.2.** Scalability analysis of two different geometries.

	Feature	Without Controller	With Controller	Remarks with respect to with controller
<b>Geometry-1</b>	Average layer height	~1.3 mm	~1.7 mm	Higher layer height
	Layers (build direction)	~193	~147	~46 lesser number of layers
	Specific energy	~74.5 J/mm <sup>3</sup>	~58.16 J/mm <sup>3</sup>	~22% improvement in process efficiency
	Total energy	~67.05 MJ	~44.63 MJ	~33.43% overall energy saved
	Part build time	~10 hr 43 min	~8 hr 10 min	~2 hr 33 min build time saved
	Volume Removed in Post Processing	~275*10 <sup>3</sup> mm <sup>3</sup>	~142.5*10 <sup>3</sup> mm <sup>3</sup>	~1.04 kg wire material (or ~262 m length) was saved
	Mass of material removed	~2.16 kg	~1.12 kg	
<b>Geometry-2</b>	Average layer height	~1.3 mm	~1.7 mm	Higher layer height
	Layers (build direction)	~193	~147	~46 lesser number of layers in the build direction
	Layers (orthogonal to scan direction)	~23	~27	~4 additional layers in adjacent to the scan direction
	Total no. Layers	193*23 = 4439	147*27 = 3969	~470 Lesser layers
	Specific energy	~74.5 J/mm <sup>3</sup>	~58.16 J/mm <sup>3</sup>	~22% improvement in process efficiency
	Total energy	~951.74 MJ	~740.82 MJ	~22.16% overall energy saved
	Part build time	~246 hr 36 min	~220 hr 30 min	~26 hr 6 min build time saved
	Volume removed in post processing	500 x 250 x (102.2-100) ~275*10 <sup>3</sup> mm <sup>3</sup>	500 x 250 x (101.9-100) ~237.5*10 <sup>3</sup> mm <sup>3</sup>	~0.3 kg wire material (or ~76 m length) was saved.
	Mass of material removed	~2.16 kg	~1.86 kg	

Overall, the implementation of a temperature-dependent feedback-based control system offers substantial advantages in additive manufacturing applications. It enhances process stability, improves energy efficiency, and ensures consistent mechanical properties across multilayer depositions. The scalability analysis confirms that this system could be successfully extended to industrial applications for the fabrication of medium to large parts.

## **4.5 Summary**

This chapter shows the successful implementation of the closed-loop feedback-based control system and a detailed analysis of the various geometrical, microstructural, and mechanical properties. A comparative study was performed between with and without controlled deposition. Further, a theoretical scalability analysis was also conducted to evaluate the feasibility of the feedback-based control system for large-scale component fabrication.

## Chapter 5 Conclusions

This dissertation devotes an experimental investigation of the close-loop-based feedback control system and its successful implementation in WAAM-TIG. It was focused on identifying its impact on process efficiency, bead geometry, thermal stability, and mechanical properties. The developed control system incorporated a PID controller to regulate the input current, ensuring stable deposition temperatures and preventing overheating during multilayer bead deposition. The recorded current, voltage, and temperature profiles demonstrated that the system effectively maintained process stability while significantly improving deposition consistency.

*The major contributions of this thesis could be identified as follows.*

- Enhanced process stability and uniformity: real-time temperature monitoring and its regulation enables the more stable and uniform bead deposition across layers, ensuring consistent process performance. The implemented feedback control system helped to maintain the uniform thermal condition and improved the overall deposition quality.
- Improvement in process efficiency: About 22% improvement in process efficiency was achieved with the proposed feedback-based controlled system. This efficiency gain was primarily attributed to optimised energy utilisation, where the system precisely regulated the energy input to prevent excessive heat accumulation while maintaining a steady deposition.
- Bead geometry analysis: For multilayered walls, more uniformity in the bead profile was observed with the proposed system. Also, an increase in height of  $\sim 27.1\%$  and a decrease in width of  $\sim 14.7\%$  was observed which would be advantageous for the fabrication of thin-walled larger components. This finding could be helpful to fabricate high-aspect-ratio structures with efficient material utilisation while maintaining structural integrity.
- The system does not show any adverse effect of controlled temperature deposition as evident from the analysed properties such as hardness, microstructure, and strength, which fell in similar ranges. This indicates that thermal control does not compromise material performance, making the

system viable for industrial applications where precision and reliability are critical.

## **5.2 Future work**

- The conducted experimental research could be extended in future to investigate the effect of controlled temperature deposition on the other mechanical properties, such as fatigue resistance and residual stresses, to enhance structural reliability.
- The work could also be extended for other materials of engineering interest.
- Further, enhancing real-time monitoring through advanced sensing technologies and AI-driven adaptive control could be attempted to improve precision.

These advancements may drive automation, efficiency, and broader industrial adoption of this proposed closed loop-based feedback control system.

## References

- [1] J. S. Panchagnula and S. Simhambhatla, "Manufacture of complex thin-walled metallic objects using weld-deposition based additive manufacturing," *Robot Comput Integr Manuf*, vol. 49, pp. 194–203, Feb. 2018, doi: 10.1016/j.rcim.2017.06.003.
- [2] B. Wu *et al.*, "A review of the wire arc additive manufacturing of metals: properties, defects and quality improvement," Oct. 01, 2018, *Elsevier Ltd.* doi: 10.1016/j.jmapro.2018.08.001.
- [3] A. F. Norman, V. Drazhner, and P. B. Prangnell, "Effect of welding parameters on the solidification microstructure of autogenous TIG welds in an Al-Cu-Mg-Mn alloy," 1999.
- [4] D. Jafari, T. H. J. Vaneker, and I. Gibson, "Wire and arc additive manufacturing: Opportunities and challenges to control the quality and accuracy of manufactured parts," *Mater Des*, vol. 202, Apr. 2021, doi: 10.1016/j.matdes.2021.109471.
- [5] C. Xia *et al.*, "A review on wire arc additive manufacturing: Monitoring, control and a framework of automated system," Oct. 01, 2020, *Elsevier B.V.* doi: 10.1016/j.jmsy.2020.08.008.
- [6] J.-H. Song, W.-K. Jung, and S.-H. Ahn, "Improved Energy Efficiency of Laser-Enhanced Nanoparticle Deposition System Analyzed with a Smart Power Monitoring Device," *International Journal of Precision Engineering and Manufacturing-Green Technology*, vol. 10, no. 3, pp. 747–756, May 2023, doi: 10.1007/s40684-022-00494-0.
- [7] Y. Yang, Y. Wang, Q. Liao, J. Pan, J. Meng, and H. Huang, "CNC Corner Milling Parameters Optimization Based on Variable-Fidelity Metamodel and Improved MOPSO Regarding Energy Consumption," *International Journal of Precision Engineering and Manufacturing-Green Technology*, vol. 9, no. 4, pp. 977–995, Jul. 2022, doi: 10.1007/s40684-021-00338-3.
- [8] V. Kumar, M. K. Parida, and S. K. Albert, "The state-of-the-art methodologies for quality analysis of arc welding process using weld data acquisition and analysis techniques," Feb. 01, 2022, *Springer*. doi: 10.1007/s13198-021-01282-w.
- [9] A. Lebar, L. Selak, R. Vrabčič, and P. Butala, "Online monitoring, analysis, and remote recording of welding parameters to the welding diary," *Strojniski Vestnik/Journal of Mechanical Engineering*, vol. 58, no. 7–8, pp. 444–452, 2012, doi: 10.5545/sv-jme.2012.341.
- [10] C. Xia *et al.*, "Model predictive control of layer width in wire arc additive manufacturing," *J Manuf Process*, vol. 58, pp. 179–186, Oct. 2020, doi: 10.1016/j.jmapro.2020.07.060.
- [11] N. Ana Rosli, M. Rizal Alkahari, F. Redza Ramli, M. Nizam Sudin, and S. Maidin, "Influence of Process Parameters in Wire and Arc Additive Manufacturing (WAAM) Process," *Journal of Mechanical Engineering*, vol. 17, no. 2, pp. 69–78, 2020.
- [12] K. Dai, W. Jiao, J. Wang, and F. Zhang, "The research of adaptive PID for the thin-walled cylinder TIG welding penetration control," in *2010 International Conference*

on Computing, Control and Industrial Engineering, CCIE 2010, 2010, pp. 30–33. doi: 10.1109/CCIE.2010.15.

- [13] D. Baier, F. Wolf, T. Weckenmann, M. Lehmann, and M. F. Zaeh, “Thermal process monitoring and control for a near-net-shape Wire and Arc Additive Manufacturing,” *Production Engineering*, vol. 16, no. 6, pp. 811–822, Dec. 2022, doi: 10.1007/s11740-022-01138-7.
- [14] Y. Wang *et al.*, “Coordinated monitoring and control method of deposited layer width and reinforcement in WAAM process,” *J Manuf Process*, vol. 71, pp. 306–316, Nov. 2021, doi: 10.1016/j.jmapro.2021.09.033.
- [15] V. L. Jorge, F. R. Teixeira, and A. Scotti, “Pyrometrical Interlayer Temperature Measurement in WAAM of Thin Wall: Strategies, Limitations and Functionality,” *Metals (Basel)*, vol. 12, no. 5, May 2022, doi: 10.3390/met12050765.
- [16] B. Wu, Z. Pan, D. Ding, D. Cuiuri, and H. Li, “Effects of heat accumulation on microstructure and mechanical properties of Ti6Al4V alloy deposited by wire arc additive manufacturing,” *Addit Manuf*, vol. 23, pp. 151–160, Oct. 2018, doi: 10.1016/j.addma.2018.08.004.
- [17] N. A. Rosli, M. R. Alkahari, M. F. bin Abdollah, S. Maidin, F. R. Ramli, and S. G. Herawan, “Review on effect of heat input for wire arc additive manufacturing process,” 2021, *Elsevier Editora Ltda*. doi: 10.1016/j.jmrt.2021.02.002.
- [18] C. Su, X. Chen, C. Gao, and Y. Wang, “Effect of heat input on microstructure and mechanical properties of Al-Mg alloys fabricated by WAAM,” *Appl Surf Sci*, vol. 486, pp. 431–440, Aug. 2019, doi: 10.1016/j.apsusc.2019.04.255.
- [19] B. Wu *et al.*, “Effects of heat accumulation on the arc characteristics and metal transfer behavior in Wire Arc Additive Manufacturing of Ti6Al4V,” *J Mater Process Technol*, vol. 250, pp. 304–312, Dec. 2017, doi: 10.1016/j.jmatprotec.2017.07.037.
- [20] A. U. Khan, M. Patidar, and Y. K. Madhukar, “In-Situ Temperature Monitoring and Feedback Control in the Gas Tungsten Arc Welding Process,” *International Journal of Precision Engineering and Manufacturing*, vol. 23, no. 12, pp. 1367–1380, Dec. 2022, doi: 10.1007/s12541-022-00704-4.
- [21] A. U. Khan and Y. K. Madhukar, “An Economic Design and Development of the Wire Arc Additive Manufacturing Setup,” in *Procedia CIRP*, Elsevier B.V., 2020, pp. 182–187. doi: 10.1016/j.procir.2020.02.166.
- [22] S. Sadhya, A. U. Khan, A. Kumar, S. Chatterjee, and Y. K. Madhukar, “Development of concurrent multi wire feed mechanism for WAAM-TIG to enhance process efficiency,” *CIRP J Manuf Sci Technol*, vol. 51, pp. 313–323, Jul. 2024, doi: 10.1016/j.cirpj.2024.04.010.
- [23] L. Bergonzi, M. Vettori, and A. Pirondi, “Development of a miniaturized specimen to perform uniaxial tensile tests on high performance materials,” in *Procedia Structural Integrity*, Elsevier B.V., 2019, pp. 213–224. doi: 10.1016/j.prostr.2020.02.018.
- [24] C. R. Cunningham, J. M. Flynn, A. Shokrani, V. Dhokia, and S. T. Newman, “Invited review article: Strategies and processes for high quality wire arc additive manufacturing,” Aug. 01, 2018, *Elsevier B.V*. doi: 10.1016/j.addma.2018.06.020.

- [25] B. Baufeld, O. Van der Biest, and R. Gault, "Additive manufacturing of Ti-6Al-4V components by shaped metal deposition: Microstructure and mechanical properties," *Mater Des*, vol. 31, no. SUPPL. 1, Jun. 2010, doi: 10.1016/j.matdes.2009.11.032.
- [26] J. L. Prado-Cerqueira *et al.*, "Analysis of favorable process conditions for the manufacturing of thin-wall pieces of mild steel obtained by wire and arc additive manufacturing (WAAM)," *Materials*, vol. 11, no. 8, Aug. 2018, doi: 10.3390/ma11081449.
- [27] S. Liu *et al.*, "Mechanical Performance of ER70S-6 Low-Carbon Steel Fabricated by Wire Arc Additive Manufacturing," Research Publishing Services, Jan. 2023, pp. 79–85. doi: 10.3850/978-981-18-6021-8\_or-01-0075.html.
- [28] J. H. Kong and S. W. Lee, "Development of Melt-pool Monitoring System based on Degree of Irregularity for Defect Diagnosis of Directed Energy Deposition Process," *International Journal of Precision Engineering and Manufacturing-Smart Technology*, vol. 1, no. 2, pp. 137–143, Jul. 2023, doi: 10.57062/ijpem-st.2023.0045.
- [29] Q. Wang *et al.*, "A Review on Energy Consumption and Efficiency of Selective Laser Melting Considering Support: Advances and Prospects," *International Journal of Precision Engineering and Manufacturing-Green Technology*, vol. 11, no. 1, pp. 259–276, Jan. 2024, doi: 10.1007/s40684-023-00542-3.
- [30] R. Prasad, D. T. Waghmare, K. Kumar, and M. Masanta, "Effect of overlapping condition on large area NiTi layer deposited on Ti-6Al-4V alloy by TIG cladding technique," *Surf Coat Technol*, vol. 385, Mar. 2020, doi: 10.1016/j.surfcoat.2020.125417.
- [31] A. U. Khan and Y. K. Madhukar, "Aptness of the swarf substrate for the additive manufacturing application," *CIRP J Manuf Sci Technol*, vol. 39, pp. 199–209, Nov. 2022, doi: 10.1016/j.cirpj.2022.08.007.